10/7-30-96 OSTI

LBNL-38825 1&2
UC-2000

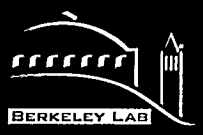

ERNEST ORLANDO LAWRENCE
BERKELEY NATIONAL LABORATORY

Two-Dimensional Analytical Solutions for Chemical Transport in Aquifers: Parts 1 and 2

C. Shan and I. Javandel
Earth Sciences Division

May 1996

Available to DOE and DOE Contractors
from the Office of Scientific and Technical Information
P.O. Box 62, Oak Ridge, TN 37831
Prices available from (615) 576-8401

Available to the public from the
National Technical Information Service
U.S. Department of Commerce
5285 Port Royal Road, Springfield, VA 22161

Ernest Orlando Lawrence Berkeley National Laboratory
is an equal opportunity employer.

LBNL-38825 1&2
UC-2000

Two-Dimensional Analytical Solutions for Chemical Transport in Aquifers

Part 1. Simplified Solutions for Sources with Constant Concentration

Part 2. Exact Solutions for Sources with Constant Flux Rate

Chao Shan and Iraj Javandel

Earth Sciences Division
Ernest Orlando Lawrence Berkeley National Laboratory
University of California
Berkeley, California 94720

May 1996

This work was supported by the Director, Office of Environmental Management, Office of Environmental Restoration, of the U.S. Department of Energy under Contract No. DE-AC03-76SF00098.

Part 1.

Simplified Solutions for Sources with Constant Concentration

Two-Dimensional Analytical Solutions for Chemical Transport in Aquifers: 1. Simplified Solutions for Sources with Constant Concentration

CHAO SHAN AND IRAJ JAVANDEL

Earth Sciences Division, Lawrence Berkeley National Laboratory

University of California, Berkeley

Berkeley, CA 94720, USA

Analytical solutions are developed for modeling solute transport in a vertical section of a homogeneous aquifer. Part 1 of the series presents a simplified analytical solution for cases in which a constant-concentration source is located at the top (or the bottom) of the aquifer. The following transport mechanisms have been considered: advection (in the horizontal direction), transverse dispersion (in the vertical direction), adsorption, and biodegradation. In the simplified solution, however, longitudinal dispersion is assumed to be relatively insignificant with respect to advection, and has been neglected. Example calculations are given to show the movement of the contamination front, the development of concentration profiles, the mass transfer rate, and an application to determine the vertical dispersivity. The analytical solution developed in this study can be a useful tool in designing an appropriate monitoring system and an effective groundwater remediation method.

INTRODUCTION

The remediation of groundwater contamination usually requires a quantitative knowledge about the distribution and fate of the contaminant. This kind of knowledge can be obtained by means of mathematical modeling which solves the advection/dispersion equation either analytically or numerically. To date, many numerical models have been developed for simulating transport problems under different initial and boundary conditions [e.g., *Pickens and Lennox*, 1976; *Sudicky*, 1989; *Yeh*, 1990]. For simplified cases, however, analytical solutions are still useful tools in practical applications.

Analytical solutions for groundwater transport can be classified into categories according to: (a) flow - a radial flow [e.g., *Chen*, 1987; *Tang and Peaceman*, 1987], or a simple one-dimensional flow; and (b) medium - a fractured porous medium [e.g., *Tang et al.*, 1981; *Sudicky and Frind*, 1982], a composite medium [e.g., *Chen*, 1991; *Tang and Aral*, 1992], or a simple homogeneous porous medium. Like most of the previous studies, the studies presented here will concentrate on problems of transport in a homogeneous aquifer with steady uniform horizontal groundwater flow.

In the literature, many analytical solutions for one-dimensional transport problems consider dispersion in the flow direction only [e.g., *van Genuchten and Alves*, 1982], while others consider two- and three-dimensional dispersions [e.g., *Cleary and Ungs*, 1978; *Wilson and Miller*, 1978; *Javandel et al*, 1984; *Domenico and Robbins*, 1985; *Leij et al*, 1991]. Almost all analytical solutions assume a uniform initial concentration and an infinite or semi-infinite medium. The contamination source can be a point, a line, a plane, or even a spatially distributed source with a constant flux rate of known value. However, there is a source characteristic that is common to all the previous studies: the source face is perpendicular to the flow direction. In reality, there are many cases where the contamination is introduced from a source at the top (or bottom) of the aquifer, whose face is parallel to the direction of groundwater flow. One typical example is the leachate from a landfill or waste site. The other is a nonaqueous-phase liquid (NAPL) sitting either on the top (light NAPL) or at the bottom (dense NAPL) of the aquifer. For

both examples, the concentration profile will be non-uniform in the vertical direction. It is the purpose of this study to obtain analytical solutions for such profiles under two different source conditions: (1) a constant concentration of known value at the source (part 1), and (2) a constant flux rate of known value from the source [part 2, *Shan and Javandel*, 1996].

Part 1 of the series applies to the problem of NAPL dissolution and transport in unconfined aquifers. Previous studies have shown that the rate of NAPL dissolution is directly related to groundwater velocity, grain size of the medium and NAPL saturation [*Miller et al.*, 1990; *Powers et al.*, 1994]. For certain aquifers with constant groundwater velocity, the concentration at the source can be a constant for certain period of time. The problem of NAPL dissolution and transport has been studied by some other researchers [*Morin et al.*, 1988; *Dillon*,1989; *Anderson et al.*, 1992a, b; *Borden and Piwoni*, 1992; *Johnson and Pankow*, 1992]. *Dillon* (1989) developed a model, DIVAST, containing three separate components: a hydraulic model, a longitudinal contaminant transport model, and a transverse contaminant diffusion model. Basically, the model applied available analytical solutions to approximate the transport in a curved flow field, which is useful to simulate transport process under the influence of a significant amount of recharge from the top of the aquifer. In a series of papers, *Anderson* and his colleagues presented their research results on the dissolution and transport of dense chlorinated solvents in groundwater. Similar studies to the part 1 subject were given by *Shan et al.* (1990). In part 1 of the series, we will present the analytical solutions systematically and focus applications on the movement of the contamination front, the concentration profiles at different locations, the mass transfer rate, and the determination of the vertical dispersivity.

THEORY

To simplify a practical problem, we give the following assumptions: (1) the aquifer is homogeneous and has a uniform thickness, h'; (2) the recharge rate in the vertical direction is insignificant such that the flow is in the horizontal direction with an average pore velocity, v'; (3) the contamination source extends uniformly to a large distance in the direction perpendicular to groundwater flow. The last assumption is necessary to simplify the problem to a vertical section. In part 1, we will neglect dispersion in the flow direction. Figure 1 shows a schematic diagram of the mathematical model, where we set the x' axis at the water table and the z' axis vertically downward. The system is divided into two regions by the z' axis: Region 1 ($-\ell' \le x' \le 0$), and Region 2 ($0 \le x' < +\infty$), where ℓ' is the length of the source in the flow direction. The dimensionless governing equations for the two regions can be written in a unified form:

$$\frac{\partial C_n}{\partial t} + \lambda C_n + \frac{\partial C_n}{\partial x} - \alpha_z \frac{\partial^2 C_n}{\partial z^2} = 0 \qquad n=1,2 \tag{1}$$

where the dimensionless variables and parameters are defined by

$$C_n = C'_n / C'_0 \tag{2}$$

$$x = \frac{x'}{\ell'}, \qquad z = \frac{z'}{\ell'}, \qquad h = \frac{h'}{\ell'}, \qquad \alpha_z = \frac{\alpha'_z}{\ell'} \tag{3}$$

$$t = \frac{v' t'}{R' \ell'}, \qquad \lambda = \frac{R' \ell' \lambda'}{v'} \tag{4}$$

where C'_n (n=1,2) represent the concentrations in Regions 1 and 2, respectively, C'_0 is the constant source concentration, t' is time, λ' is the decay constant, R' is the retardation factor, and α'_z is the "apparent dispersivity" in the vertical direction which represents the combined effect of mechanical dispersion and molecular diffusion. We will simply call α'_z the "vertical dispersivity" in the following.

The dimensionless initial and boundary conditions are assumed as follows:

$$C_n(x,z,0) = 0 \tag{5}$$

$$C_1(x,0,t) = 1 \tag{6}$$

$$C_1(-1,z,t) = 0 \tag{7}$$

$$\frac{\partial C_2(x,0,t)}{\partial z} = 0 \tag{8}$$

$$C_2(\infty,z,t) = 0 \tag{9}$$

$$C_1(0,z,t) = C_2(0,z,t) \tag{10}$$

$$\frac{\partial C_1(0,z,t)}{\partial x} = \frac{\partial C_2(0,z,t)}{\partial x} \tag{11}$$

It is probably worthwhile to point out that (7) is derived based on the assumption of "no horizontal dispersion". This assumption is given for two reasons: (a) the transport in the horizontal direction due to dispersion is usually much smaller than that due to advection; and (b) the neglect of the horizontal dispersion can simplify the solution derivation. The boundary condition at the bottom of the aquifer ($z'=h'$) has not been given because we want to solve the problem for two different cases.

Case 1. Infinite h'

For this case, we assume that h' is so large that the contaminant front will not reach the bottom of the aquifer in the time period of interest. Under this assumption we may use the following boundary condition

$$C_n(x,\infty,t) = 0 \tag{12}$$

With a complete set of conditions, we now solve (1) in both regions separately.

Region 1

Applying the Laplace transform with respect to t and the Fourier sine transform with respect to z, consecutively, (1) is reduced to

$$\frac{dC_{1LF}}{dx} + (s + \lambda + \alpha_z r^2) C_{1LF} = \frac{\alpha_z r}{s} \tag{13}$$

where s and r are the Laplace transform and the Fourier sine transform parameters, respectively, and C_{1LF} is defined by

$$C_{1LF}(x,r,s) = \int_0^\infty C_{1L}(x,z,s)\sin(rz)dz \tag{14}$$

$$C_{1L}(x,z,s) = \int_0^\infty C_1(x,z,t)e^{-st}dt \tag{15}$$

The solution of (13) that satisfies boundary condition (7) in the transformed domain is

$$C_{1LF}(x,r,s) = \frac{\alpha_z r}{s(s + \lambda + \alpha_z r^2)}\left[1 - e^{-(s+\lambda+\alpha_z r^2)(x+1)}\right] \tag{16}$$

For (16), if we take the inverse Laplace transform with respect to s and the inverse Fourier sine transform with respect to r, consecutively, we obtain

$$C_1(x,z,t) = f(t)u(x+1-t) + f(x+1)u(t-x-1) \tag{17A}$$

where

$$f(y) = \frac{1}{2}\left[e^{-z\sqrt{\lambda/\alpha_z}}erfc\left(\frac{z}{2\sqrt{\alpha_z y}} - \sqrt{\lambda y}\right) + e^{z\sqrt{\lambda/\alpha_z}}erfc\left(\frac{z}{2\sqrt{\alpha_z y}} + \sqrt{\lambda y}\right)\right] \tag{17B}$$

and $u(y)$ is the Heaviside unit function, which is zero for $y<0$ and unity for $y>0$. The detailed derivation process is given in Appendix A.

For some cases, we may want to neglect the decay effect such that $\lambda=0$. In this circumstance, the solution for Region 1 is reduced to

$$C_1(z,t) = erfc\left(\frac{z}{2\sqrt{\alpha_z t}}\right) \qquad (t<x+1) \tag{18A}$$

$$C_1(x,z) = erfc\left(\frac{z}{2\sqrt{\alpha_z (x+1)}}\right) \qquad (t>x+1) \tag{18B}$$

It is easy to see that as $t=x+1$ the two equations give exactly the same result, and the solution reaches a steady state. The time required to reach the steady state, $x+1$, is actually the distance from the up-gradient end of the source to the location of interest. Similar analysis can be given to the rest of the solutions.

Region 2

Applying the Laplace transform twice, first with respect to t and then with respect to x, the governing equation, (1) is reduced to

$$\frac{d^2 C_{2LL}}{dz^2} - A^2 C_{2LL} = -g(z,s) \tag{19}$$

where C_{2LL}, A and $g(z,s)$ are defined by

$$C_{2LL}(p,z,s) = \int_0^\infty C_{2L}(x,z,s) e^{-px} dx \tag{20}$$

$$C_{2L}(x,z,s) = \int_0^\infty C_2(x,z,t) e^{-st} dt \tag{21}$$

$$A = \sqrt{(s+p+\lambda)/\alpha_z} \tag{22}$$

and

$$g(z,s) = \frac{1}{2s\alpha_z}\left[e^{-z\sqrt{(s+\lambda)/\alpha_z}}erfc\left(\frac{z}{2\sqrt{\alpha_z}} - \sqrt{s+\lambda}\right) + e^{z\sqrt{(s+\lambda)/\alpha_z}}erfc\left(\frac{z}{2\sqrt{\alpha_z}} + \sqrt{s+\lambda}\right)\right] \tag{23}$$

The symbols s and p are the Laplace transform parameters. Substituting (22) and (23) into (19), and solving the resulting equation, we obtain

$$C_{2LL} = g_1 - g_2 + g_3 - g_4 \tag{24}$$

$$g_1 = \frac{1}{2sp}\left[e^{-z\sqrt{(s+\lambda)/\alpha_z}}erfc\left(\frac{z}{2\sqrt{\alpha_z}} - \sqrt{s+\lambda}\right) + e^{z\sqrt{(s+\lambda)/\alpha_z}}erfc\left(\frac{z}{2\sqrt{\alpha_z}} + \sqrt{s+\lambda}\right)\right] \tag{25A}$$

$$g_2 = \frac{e^p}{2sp}\left[e^{-z\sqrt{(s+p+\lambda)/\alpha_z}}erfc\left(\frac{z}{2\sqrt{\alpha_z}} - \sqrt{s+p+\lambda}\right) + e^{z\sqrt{(s+p+\lambda)/\alpha_z}}erfc\left(\frac{z}{2\sqrt{\alpha_z}} + \sqrt{s+p+\lambda}\right)\right] \tag{25B}$$

$$g_3 = \frac{e^p}{sp}e^{-z\sqrt{(s+p+\lambda)/\alpha_z}}erf(\sqrt{s+p+\lambda}) \tag{25C}$$

$$g_4 = \frac{e^{-z\sqrt{(s+p+\lambda)/\alpha_z}}}{sp\sqrt{s+p+\lambda}}\sqrt{s+\lambda}\,erf(\sqrt{s+\lambda}) \tag{25D}$$

A double Laplace inversion leads to

$$C_2 = 0 \qquad (t<x) \tag{26A}$$

$$C_2(x,z,t) = \frac{e^{-\lambda t}}{\pi}\int_x^t \frac{e^{-z^2/(4\alpha_z\tau)}}{\sqrt{\tau(t-\tau)}}d\tau + \frac{\lambda}{\pi}\int_x^t e^{-\lambda T}dT\int_x^T \frac{e^{-z^2/(4\alpha_z\tau)}}{\sqrt{\tau(T-\tau)}}d\tau \qquad (x<t<x+1) \tag{26B}$$

$$C_2(x,z) = \frac{e^{-\lambda(x+1)}}{\pi}\int_x^{x+1} \frac{e^{-z^2/(4\alpha_z\tau)}}{\sqrt{\tau(x+1-\tau)}}d\tau + \frac{\lambda}{\pi}\int_x^{x+1} e^{-\lambda T}dT\int_x^T \frac{e^{-z^2/(4\alpha_z\tau)}}{\sqrt{\tau(T-\tau)}}d\tau \qquad (t>x+1) \tag{26C}$$

A detailed derivation process is given in Appendix A.

In cases where the decay is not considered ($\lambda=0$), the solution can be simplified to

$$C_2 = 0 \qquad (t<x) \tag{27A}$$

$$C_2(x,z,t) = \frac{1}{\pi}\int_x^t \frac{e^{-z^2/(4\alpha_z\tau)}}{\sqrt{\tau(t-\tau)}}d\tau \qquad (x<t<x+1) \tag{27B}$$

$$C_2(x,z) = \frac{1}{\pi}\int_x^{x+1} \frac{e^{-z^2/(4\alpha_z\tau)}}{\sqrt{\tau(x+1-\tau)}}d\tau \qquad (t>x+1) \tag{27C}$$

Case 2. Finite h'

For this case, boundary condition (12) is replaced by

$$\frac{\partial C_n}{\partial z}(x,h,t) = 0 \tag{28}$$

Once again, we need to solve Equation (1) in two regions consecutively.

Region 1

Applying the Laplace transform with respect to t, and the generalized finite Fourier transform with respect to z consecutively, (1) is reduced to

$$\frac{dC_{1Lf}}{dx} + (s+\lambda+\alpha_z a_n^2)C_{1Lf} = \frac{\alpha_z a_n}{s} \tag{29}$$

where

$$C_{1Lf}(x,n,s) = \int_0^h C_{1L}(x,z,s)\sin(a_n z)dz \tag{30}$$

$$a_n = \left(n-\frac{1}{2}\right)\frac{\pi}{h} \tag{31}$$

where C_{IL} is the Laplace transform defined by (15). The solution of (29) which satisfies boundary condition (7) in the transformed domain is

$$C_{1Lf}(x,n,s) = \frac{\alpha_z a_n}{s(s+\lambda+\alpha_z a_n^2)}\left[1-e^{-(s+\lambda+\alpha_z a_n^2)(x+1)}\right] \tag{32}$$

Similarly, if we take the inverse Laplace transform with respect to s, and use the generalized finite Fourier inversion formula (Churchill, 1958)

$$C_1(x,z,t) = \frac{2}{h}\sum_{n=1}^{\infty} C_{1f}(x,n,t)\sin(a_n z) \tag{33}$$

we obtain the solution for Region 1:

$$C_1(x,z,t) = u(x+1-t)\frac{2}{h}\sum_{n=1}^{\infty} f_n(t)\sin(a_n z) + u(t-x-1)\frac{2}{h}\sum_{n=1}^{\infty} f_n(x+1)\sin(a_n z) \tag{34A}$$

where

$$f_n(y) = \frac{\alpha_z a_n}{\alpha_z a_n^2+\lambda}\left[1-e^{-(\alpha_z a_n^2+\lambda)y}\right] \tag{34B}$$

Region 2

Applying the Laplace transform with respect to t, and the finite Fourier cosine transform with respect to z consecutively, (1) is reduced to

$$\frac{dC_{2Lf}}{dx} + (s+\lambda+\alpha_z b_m^2)C_{2Lf} = 0 \tag{35}$$

where

$$C_{2Lf}(x,m,s) = \int_0^h C_{2L}(x,z,s)\cos(b_m z)\,dz \tag{36}$$

$$b_m = \frac{m\pi}{h} \tag{37}$$

where C_{2L} is the Laplace transform defined by (21). The general solution to (35) is

$$C_{2Lf}(x,m,s) = ke^{-(s+\lambda+\alpha_z b_m^2)x} \tag{38}$$

where k is an integral constant determined as

$$k = C_{2Lf}(0,m,s) = \frac{2}{h}\sum_{n=1}^{\infty} \frac{\alpha_z a_n^2}{a_n^2 - b_m^2} \cdot \frac{1 - e^{-(s+\lambda+\alpha_z a_n^2)}}{s(s+\lambda+\alpha_z a_n^2)} \tag{39}$$

Several steps are required to obtain (39): (a) set $x=0$ in (38); (b) apply (36) at $x=0$; (c) apply (10) in the Laplace transformed domain to obtain $C_{2L}(0,z,s)=C_{1L}(0,z,s)$; (d) apply (33) to (32) and set $x=0$ to calculate $C_{1L}(0,z,s)$; and (e) substitute $C_{1L}(0,z,s)$ into (36) and integrate.

Similarly, if we take the inverse Laplace transform with respect to s, we obtain

$$C_{2f} = 0 \qquad (t<x) \tag{40A}$$

$$C_{2f}(x,m,t) = \frac{2}{h}\sum_{n=1}^{\infty} \frac{\alpha_z a_n^2}{a_n^2 - b_m^2} \cdot \frac{1 - e^{-(\lambda+\alpha_z a_n^2)(t-x)}}{\lambda+\alpha_z a_n^2} \cdot e^{-(\lambda+\alpha_z b_m^2)x} \qquad (x<t<x+1) \tag{40B}$$

$$C_{2f}(x,m) = \frac{2}{h}\sum_{n=1}^{\infty} \frac{\alpha_z a_n^2}{a_n^2 - b_m^2} \cdot \frac{1 - e^{-(\lambda+\alpha_z a_n^2)}}{\lambda+\alpha_z a_n^2} \cdot e^{-(\lambda+\alpha_z b_m^2)x} \qquad (t>x+1) \tag{40C}$$

Finally, we apply the inversion formula for the finite Fourier cosine transform (Churchill, 1958)

$$C_2(x,z,t) = \frac{1}{h}C_{2f}(x,0,t) + \frac{2}{h}\sum_{m=1}^{\infty} C_{2f}(x,m,t)\cos(b_m z) \tag{41}$$

and obtain

$$C_2 = 0 \qquad (t<x) \tag{42A}$$

$$C_2(x,z,t) = \frac{2\alpha_z e^{-\lambda x}}{h^2}\sum_{n=1}^{\infty}\frac{1-e^{-(\lambda+\alpha_z a_n^2)(t-x)}}{\lambda+\alpha_z a_n^2} + \frac{4}{h^2}\sum_{m=1}^{\infty}\cos(b_m z)\sum_{n=1}^{\infty}\frac{\alpha_z a_n^2}{a_n^2-b_m^2}\cdot\frac{1-e^{-(\lambda+\alpha_z a_n^2)(t-x)}}{\lambda+\alpha_z a_n^2}\cdot e^{-(\lambda+\alpha_z b_m^2)x}$$

$$(x<t<x+1) \tag{42B}$$

$$C_2(x,z) = \frac{2\alpha_z e^{-\lambda x}}{h^2}\sum_{n=1}^{\infty}\frac{1-e^{-(\lambda+\alpha_z a_n^2)}}{\lambda+\alpha_z a_n^2} + \frac{4}{h^2}\sum_{m=1}^{\infty}\cos(b_m z)\sum_{n=1}^{\infty}\frac{\alpha_z a_n^2}{a_n^2-b_m^2}\cdot\frac{1-e^{-(\lambda+\alpha_z a_n^2)}}{\lambda+\alpha_z a_n^2}\cdot e^{-(\lambda+\alpha_z b_m^2)x}$$

$$(t>x+1) \tag{42C}$$

We find that the steady solution, (42C) can be obtained by setting $t=x+1$ in the transient solution, (42B).

RESULTS AND APPLICATIONS

The two solutions derived for the two cases (finite or infinite aquifer thickness) both contain a transient part for $t<x+1$ and a steady-state part for $t\geq x+1$. In both Region 1 ($x<0$) and Region 2 ($x>0$), for the case of no retardation ($R'=1$), the time to reach steady state represents the groundwater travel time from the fresh water entry (at $x=-1$) to the point of calculation. In Region 2, both solutions give a zero concentration for $t<x$. The reason is that Region 2 receives contaminants from Region 1 only through advection.

The two solutions each have advantages and disadvantages. The solution for the case of an infinite aquifer thickness requires a numerical integration and a double check to make sure that the contamination front has not reached the bottom of the aquifer; however, the solution has a simple form and is easy to calculate with a computer program. The solution for the case of a finite aquifer thickness does not need

a numerical integration and is always applicable for aquifers with small thickness; however, the solution is accurate only if sufficiently large number of terms are taken from the infinite series. If the point of calculation is very close to either the upper or lower boundary, more terms are needed to achieve a high accuracy (note: the finite thickness solution cannot be used to calculate the concentrations at $z=0$ and $z=h$). A comparison of the two solutions is given in Figure 2, for $\lambda=0$, $\alpha_z=0.001$ and $t=10$. The solid lines represent the relative concentration contours calculated using the infinite thickness solution; and the dots represent the corresponding concentration calculated using the finite thickness solution with $h=0.5$. Since the contamination front ($C=0.001$) has not reached the bottom of the aquifer at the time of calculation ($t=10$), the two solutions give almost the same results. In calculating the finite thickness solution, we have used up to 1000 terms in Region 1, 50 terms for m and 100 terms for n in Region 2. Further increase of these numbers has an insignificant effect on the results. In reality, the length of the source can be on the order of tens or hundreds of meters, while the vertical dispersivity can be on the order of centimeters or millimeters. As a result, the dimensionless dispersivity, α_z can be smaller than 0.001. For convenience, we assume $\lambda=0$, $\alpha_z=0.001$ (except for the study of dispersivity effect) and use the infinite thickness solution for the following study of applications.

Mass Transfer Rates

In practice, it is important to estimate the mass transfer rate of a specific chemical from the NAPL source to the aquifer. Using the solution for the infinite thickness case at Region 1 (equations 18A and 18B), the mass transfer rate can be calculated by (a detailed derivation is given in Appendix A):

$$M_z = \frac{1}{\sqrt{\pi \alpha_z}}\left(\sqrt{t} + \frac{1}{\sqrt{t}}\right) \qquad (t<1) \qquad (43A)$$

$$M_z = \frac{2}{\sqrt{\pi \alpha_z}} \qquad (t \geq 1) \qquad (43B)$$

where the dimensionless mass transfer rate, M_z is defined as

$$M_z = \frac{M'_z}{v' \alpha'_z C'_0} \qquad (44)$$

where M'_z is the mass transfer rate per unit width of NAPL.

The mass transfer rate of a given solute in groundwater can also be estimated across any vertical section in the aquifer. A section of particular interest is the interface between Regions 1 and 2, at $x=0$. This mass transfer rate can be calculated by (a detailed derivation is given in Appendix A):

$$M_x = \frac{2\sqrt{t}}{\sqrt{\pi \alpha_z}} \qquad (t<1) \qquad (45A)$$

$$M_x = \frac{2}{\sqrt{\pi \alpha_z}} \qquad (t \geq 1) \qquad (45B)$$

where the dimensionless mass transfer rate, M_x is defined by

$$M_x = \frac{M'_x}{v' \alpha'_z C'_0} \qquad (46)$$

where M'_x is the mass transfer rate per unit width of aquifer.

The variation of the normalized mass transfer rates is given in Figure 3, where the normalized mass transfer rates, Q_z and Q_x are defined by

$$Q_i = \frac{\sqrt{\pi \alpha_z}}{2} M_i \qquad (i=z,x) \tag{47}$$

The normalized mass release rate from the source (Q_z) starts from a relatively large value and then declines, approaching unity as the dimensionless time, t becomes 1. Thereafter, the release rate remains constant, based on the assumption of a constant NAPL supply. Depending on the initial volume of NAPL, the assumption could be valid for relatively long time, T_r, which can be estimated by

$$T_r \approx \frac{\sqrt{\pi} M_t}{2v' C_0' \sqrt{\alpha_z' \ell'}} \tag{48}$$

where M_t is the initial NAPL mass per unit width. In deriving (48), we have neglected the early time difference in mass release rate and assumed no dependence on NAPL saturation. Figure 3 also shows that the normalized mass transfer rate leaving the source area (Q_x) increase from zero at the beginning to unity at $t=1$, and remains constant later. The figure suggests that for all times corresponding to $t>1$ the mass entering the groundwater is equal to the mass leaving the source area. As a result, the mass of the contaminants in the source area, Region 1, remains constant for all values of times corresponding to $t>1$. Note that, for the case of no retardation, $t=1$ corresponds to the time (t') required for the water particles to travel the length of the NAPL (ℓ') along the groundwater-flow direction. Also note that the area confined between the curves for Q_z and Q_x in Figure 3 is a measure of the mass of the constituent finally accumulated in Region 1. By means of integration, the accumulated mass per unit width of aquifer, M_a can be estimated by

$$M_a = \frac{2}{3} R' \ell' \alpha_z' C_0' \tag{49}$$

Contamination Front

In most cases, one of our main concerns is how the contamination front moves through the aquifer. To address this concern, we need to give the definition of *contamination front* for a specific problem. For example, if the concentration of a constituent at the NAPL source is its solubility in water, and the drinking water standard is one thousandth of the solubility, then the relative concentration contour of C=0.001 is the contamination front. For α_z=0.001, the contamination front at three different times is shown in Figure 4. By means of this figure, one can find the contamination thickness at different locations, which are useful for determining the depth of the monitoring and remediation wells.

Concentration Profiles

In some other cases, we may be interested in the magnitude of contamination at different depths in a well. Figure 5 shows examples of concentration profiles at four different locations, x=*0, 1, 2, 3* using α_z=0.001. We have divided the figure into four frames using two sets of horizontal coordinates. The upper coordinate for each frame increasing from 0 to 1 represents the relative concentration, while the number shown at the lower left corner of each frame indicates the x coordinate of the profile section. Each frame refers to two values of time, and the one with larger value shows the steady-state concentration distribution. The larger value indicates the time when steady-state is reached. According to this figure, concentration at a certain point downstream from the source increases with time until it reaches steady state. This figure also shows that the depth of plume penetration increases with the distance downstream from the NAPL source and that the steady-state concentration at shallow depths decreases with distance downstream.

Determination of Vertical Dispersivity

In above applications, we have assumed that the vertical dispersivity is a known value. We now discuss how to apply the analytical solution and field data to determine the vertical dispersivity inversely.

To avoid the error caused by the estimation of time, the steady-state solution (18B and 27C) is recommended. Correspondingly, only the steady concentrations from the field data will be used. Since the functional relationship between α_z and C is implicit, one needs to determine the vertical dispersivity by using the method of iteration. As an example, we pick the location at $x=0$ so that we can apply the simple formula, (18B). Since we know C_1 and z, we can use the z value and an assumed α_z value to calculate the relative concentration using (18B). The right α_z value is the one that would give a calculated relative concentration equal to the observed value, C_1. Figure 6 shows a set of type curves corresponding to different values of z at $x=0$ for determining the vertical dispersivity.

CONCLUSION

Two analytical solutions have been derived independently for the problem of NAPL dissolution and transport in unconfined aquifers, one assuming an infinite aquifer thickness, the other using finite aquifer thickness. Both solutions consider advection in the aquifer flow direction (with constant flow rate), dispersion in the vertical direction, adsorption, and biodegradation. By comparing the two solutions, the assumption of *infinite aquifer thickness* has been proved valid as long as the contamination front does not reach the bottom of the aquifer. The solutions can be used to predict the contamination development, to calculate the mass transfer rate, and to determine the vertical dispersivity. Although the solutions were derived using a source on the top of the aquifer (representing a light NAPL case), the solutions can also be applied to cases of a source at the bottom of the aquifer (representing a dense NAPL case). In the latter case, all we need to do is simply reverse the z' axis in Figure 1 and shift the origin to the bottom of the aquifer.

ACKNOWLEDGMENT

This work was supported in part by California Department of Health Services and in part by the Director, Office of Environmental Management, Office of Environmental Restoration of the U.S. Department of Energy under contract DE-AC03-76SF00098. The authors thank D. B. Stephens for his suggestions and C. Doughty and G. Xie for reviewing the manuscript.

REFERENCES

Anderson, M. R., R. L. Johnson, and J. F. Pankow, Dissolution of dense chlorinated solvents into ground water: 1. Dissolution from a well-defined residual source, *Ground Water, 30(2)*: 250-256, 1992a.

Anderson, M. R., R. L. Johnson, and J. F. Pankow, Dissolution of dense chlorinated solvents into groundwater: 3. Modeling contaminant plumes from fingers and pools of solvent, *Environ. Sci. Technol., 26(5)*: 901-908, 1992b.

Borden, R. C., and M. D. Piwoni, Hydrocarbon dissolution and transport: a comparison of equilibrium and kinetic models, *J. Contam. Hydrol., 10*: 309-323, 1992.

Chen, C.-S., Analytical solutions for radial dispersion with Cauchy boundary at injection well, *Water Resour. Res., 23(7)*: 1217-1224, 1987.

Chen C.-S., Semianalytical solutions for radial dispersion in a three-layer leaky system, *Ground Water, 29(5)*: 663-670, 1991.

Churchill, R. V., *Operational Mathematics*, 2nd. ed. McGraw-Hill, New York, 1958.

Cleary, R. W., and M. J. Ungs, Analytical methods for ground water pollution and hydrology, *Water-Resour. Prog. Rep. 78-WR-15*, Dept. of Civ. Eng., Princeton Univ., Princeton, N. J., 1978.

Dillon, P. J., An analytical model of contaminant transport from diffuse sources in saturated porous media, *Water Resour. Res.*, *25(6)*: 1208-1218, 1989.

Domenico, P. A., and G. A. Robbins, A new method of contaminant plume analysis, *Ground Water*, *23(4)*: 476-485, 1985.

Erdélyi, A., *Tables of Integral Transforms*, McGraw-Hill Book Company, Inc., New York, 1954.

Gradshteyn, I. S. and I. M. Ryzhik, *Table of Integrals, Series, and Products*, Academic Press, Inc., Berkeley, 1980.

Javandel, I., C. Doughty, and C. F. Tsang, *Groundwater Transport: Handbook of Mathematical Models, Water Resour. Monogr. Ser.*, vol. 10, AGU, Washington, D. C., 1984.

Johnson, R. L., and J. F. Pankow, Dissolution of dense chlorinated solvents into groundwater: 2. Source functions for pools of solvent, *Environ. Sci. Technol.*, *26(5)*: 896-901, 1992.

Leij, F. J., T. H. Skaggs, and M. Th. van Genuchten, Analytical solutions for solute transport in three-dimensional semi-infinite porous media, *Water Resour. Res.*, *27(10)*: 2719-2733, 1991.

Miller, C. T., M. M. Poirier-McNeill, and A. S. Mayer, Dissolution of trapped nonaqueous phase liquids: Mass transfer characteristics, *Water Resour. Res.*, *26(11)*: 2783-2796, 1990.

Morin, K. A., J. A. Cherry, N. K. Davé, T. P. Lim, and A. J. Vivyurka, Migration of acidic groundwater seepage from uranium-tailings impoundments: 1. Field study and conceptual hydrogeochemical model, *J. Contam. Hydrol.*, *2*: 271-303, 1988.

Pickens, J. F., and W. C. Lennox, Numerical simulation of waste movement in steady groundwater systems, *Water Resour. Res.*, *12(2)*: 171-180, 1976.

Powers, S. E., L. M. Abriola, and W. J. Weber, Jr., An experimental investigation of nonaqueous phase liquid dissolution in saturated subsurface systems: Transient mass transfer rate, *Water Resour. Res.*, *30(2)*: 321-332, 1994.

Shan, C., I. Javandel, and P. A. Witherspoon, A simplified analytical solution for dissolution and transport of nonaqueous phase liquids in groundwater, *Annual Rep., Earth Science Division, Lawrence Berkeley Laboratory*, LBL-27900, UC-403, 1989.

Shan, C., and I. Javandel, Analytical solutions for solute transport in a vertical aquifer section: 2. Exact solutions for sources with constant flux rate, *Lawrence Berkeley Laboratory Rep. LBL-38825, Part 2*, 1996.

Sudicky, E. A., and E. O. Frind, Contaminant transport in fractured porous media: Analytical solutions for a system of parallel fractures, *Water Resour. Res.*, *18(6)*: 1634-1642, 1982.

Sudicky, E. A., The Laplace transform Galerkin technique: A time-continuous finite element theory and application to mass transport in groundwater, *Water Resour. Res.*, *25(8)*: 1833-1846, 1989.

Tang, D. H., E. O. Frind, and E. A. Sudicky, Contaminant transport in fractured porous media: Analytical solution for a single fracture, *Water Resour. Res.*, *17(3)*: 555-564, 1981.

Tang, D. H. E., and D. W. Peaceman, New analytical and numerical solutions for the radial convection-dispersion problem, *SPE Reservoir Eng.*, 343-359, 1987.

Tang, Y., and M. M. Aral, Contaminant transport in layered porous media, 1. General solution, *Water Resour. Res.*, *28(5)*: 555-564, 1992.

van Genuchten, M. Th., and W. J. Alves, Analytical solutions of the one-dimensional convective-dispersive solute transport equation, *Tech. Bull. U.S. Dep. Agric.*, *1661*, 1982.

Wilson, J. L., and P. L. Miller, Two-dimensional plume in uniform ground-water flow, *J. Hydraul. Div. Proc. Am. Soc. Civ. Eng.*, *104(HY4)*: 503-514, 1978.

Yeh, G. T., A Lagrangian-Eulerian method for zoomable hidden fine-mesh approach to solving advection-dispersion equations, *Water Resour. Res.*, *26(6)*: 1133-1144, 1990.

APPENDIX A: SOLUTION DERIVATIONS

We use the following formulae from *Tables of Integral Transforms* [*Erdélyi*, 1954].

$$\mathcal{L}^{-1}\{\phi(s+a)\} = e^{-at}\mathcal{L}^{-1}\{\phi(s)\} \tag{A1A}$$

$$\mathcal{L}^{-1}\left\{\frac{1}{s(s+a)}\right\} = (1-e^{-at})/a \tag{A1B}$$

$$\mathcal{L}^{-1}\left\{\frac{e^{-as}}{s+b}\right\} = e^{-b(t-a)}u(t-a) \tag{A1C}$$

$$\mathcal{L}^{-1}\{e^{-as}\} = \delta(t-a) \tag{A1D}$$

$$\mathcal{L}^{-1}\left\{\frac{s+a}{s}\right\} = \delta(t)+a \tag{A1E}$$

$$\mathcal{L}^{-1}\left\{\frac{erf(\sqrt{as})}{\sqrt{s}}\right\} = \frac{1}{\sqrt{\pi t}}u(a-t) \tag{A1F}$$

$$\mathcal{L}^{-1}\left\{\frac{e^{-a\sqrt{s}}}{\sqrt{s}}\right\} = \frac{1}{\sqrt{\pi t}}e^{-a^2/(4t)} \tag{A1G}$$

$$\mathcal{F}_s^{-1}\left\{\frac{r}{r^2+a^2}\right\} = e^{-az} \tag{A1H}$$

$$\mathcal{F}_s^{-1}\left\{\frac{2re^{-b^2(r^2+a^2)}}{r^2+a^2}\right\} = e^{-az}erfc(ab-\frac{z}{2b}) - e^{az}erfc(ab+\frac{z}{2b}) \tag{A1I}$$

where $u(t-a)$ is the Heaviside unit function; and $\delta(t-a)$ is the Dirac δ function. In the applications of (A1C) and (A1D) we have extended the original condition of $a>0$ to all real values of a. This can be easily proved by applying the following theorem with $b=2a$.

Theorem: If $\mathcal{L}^{-1}\{\phi(s)\}=f(t)$, *then* $\mathcal{L}^{-1}\{e^{bs}\phi(s)\}=f(t+b)$.

Derivation of (17A) and (17B)

For Equation (16), if we take the inverse Laplace transform with respect to s, we obtain

$$C_{1F} = \frac{\alpha_z r}{\alpha_z r^2+\lambda}\left[1-e^{-(\alpha_z r^2+\lambda)t}\right] \qquad (t<x+1) \tag{A2A}$$

$$C_{1F} = \frac{\alpha_z r}{\alpha_z r^2+\lambda}\left[1-e^{-(\alpha_z r^2+\lambda)(x+1)}\right] \qquad (t>x+1) \tag{A2B}$$

In this derivation, we have split (16) into three terms and applied (A1B) once, (A1C) twice, and used the definition of the Heaviside unit function. It is interesting to find that t in (A2A) was replaced by $x+1$ in (A2B).

Taking the inverse Fourier sine transform with respect to r for (A2A) and (A2B), we obtain the solutions, (17A) and (17B), in which process we have used (A1H), (A1I) and the following relationship.

$$2-erfc(b-a) = erfc(a-b) \tag{A3}$$

Derivation of (26A) through (26C)

For Equation (16) if we apply (A1H) and (A1I) to perform the inverse Fourier sine transform first, then take the inverse Laplace transform, and equate it with the results (C_I) shown in (17A) and (17B), we derive the following useful Laplace inversion formula

$$\mathcal{L}^{-1}\left\{\frac{1}{2s}\left[e^{-z\sqrt{(s+\lambda)/\alpha_z}}erfc\left(\frac{z}{2\sqrt{\alpha_z a}}-\sqrt{(s+\lambda)a}\right)+e^{z\sqrt{(s+\lambda)/\alpha_z}}erfc\left(\frac{z}{2\sqrt{\alpha_z a}}+\sqrt{(s+\lambda)a}\right)\right]\right\} =$$

$$f(t)u(a-t)+f(a)u(t-a) \tag{A4}$$

where $f(y)$ is defined by (17B). In the above process, we have replaced the term $x+1$ by a for more general application.

In fact, the inverse Fourier sine transform of (16) also allows us to obtain the Laplace transform of C_2 at $x=0$. Using boundary condition (10) and the inverse Fourier sine transform result shown in the brace of (A4), we obtain

$$C_{2L}(0,z,s) = C_{1L}(0,z,s) = \alpha_z \cdot g(z,s) \tag{A5}$$

where the function, $g(z,s)$ is defined by (23).

In solving Equation (19) to obtain the solution (24) and (25), We have used the following integration formula which was derived using the technique of integrating by parts.

$$\int e^{ax} efrc(bx+c)\,dx = \frac{1}{a}\left[e^{ax} erfc(bx+c) + e^{a^2/(4b^2)-ac/b} erf(bx+c-\frac{a}{2b})\right] \tag{A6}$$

The transformed solution, (24) is composed of four terms given in (25A) through (25D). Using (A4), the inversion of (25A) is

$$\mathcal{L}_p^{-1}\{\mathcal{L}_s^{-1}\{g_1\}\} = f(t)u(1-t) + f(1)u(t-1) \tag{A7}$$

For (25B), we first apply (A4) with respect to s, replacing λ by $p+\lambda$, and using $a=1$. We obtain

$$\mathcal{L}_s^{-1}\{g_2\} = \frac{e^p}{2p}\left[e^{-z\sqrt{(p+\lambda)/\alpha_z}} erfc\left(\frac{z}{2\sqrt{\alpha_z t}} - \sqrt{(p+\lambda)t}\right) + e^{z\sqrt{(p+\lambda)/\alpha_z}} erfc\left(\frac{z}{2\sqrt{\alpha_z t}} + \sqrt{(p+\lambda)t}\right)\right]u(1-t) +$$

$$\frac{e^p}{2p}\left[e^{-z\sqrt{(p+\lambda)/\alpha_z}} erfc\left(\frac{z}{2\sqrt{\alpha_z}} - \sqrt{(p+\lambda)}\right) + e^{z\sqrt{(p+\lambda)/\alpha_z}} erfc\left(\frac{z}{2\sqrt{\alpha_z}} + \sqrt{(p+\lambda)}\right)\right]u(t-1) \tag{A8}$$

If we further apply (A4) to (A8) with respect to p and use the theorem, we obtain

$$\mathcal{L}_p^{-1}\{\mathcal{L}_s^{-1}\{g_2\}\} = [f(x+1)u(t-x-1) + f(t)u(x+1-t)]u(1-t) + [f(x+1)u(-x) + f(1)u(x)]u(t-1) \tag{A9}$$

Noting that $x>0$ in Region 2, by using the definition of the Heaviside unit function, we obtain the inversion for g_2, which is exactly the same as (A7).

$$\mathcal{L}_p^{-1}\{\mathcal{L}_s^{-1}\{g_2\}\} = f(t)u(1-t) + f(1)u(t-1) \tag{A10}$$

To obtain the inversion for (25C) we first rewrite it as

$$g_3 = \frac{e^p}{p} \cdot \frac{s+p+\lambda}{s} \cdot \frac{e^{-z\sqrt{(s+p+\lambda)/\alpha_z}}}{s+p+\lambda} erf(\sqrt{s+p+\lambda}) \tag{A11}$$

By applying (A1E) through (A1G) we obtain

$$\mathcal{L}^{-1}\left\{\frac{s+p+\lambda}{s}\right\} = \delta(t) + (p+\lambda) \tag{A12}$$

$$\mathcal{L}^{-1}\left\{\frac{erf(\sqrt{s})}{\sqrt{s}}\right\} = \frac{1}{\sqrt{\pi t}} u(1-t) \tag{A13}$$

$$\mathcal{L}^{-1}\left\{\frac{e^{-z\sqrt{s/\alpha_z}}}{\sqrt{s}}\right\} = \frac{1}{\sqrt{\pi t}} e^{-z^2/(4\alpha_z t)} \tag{A14}$$

Applying (A1A) and the convolution theorem, we obtain

$$\mathcal{L}_s^{-1}\left\{\frac{e^{-z\sqrt{(s+p+\lambda)/\alpha_z}}}{s+p+\lambda} erf(\sqrt{s+p+\lambda})\right\} = \frac{e^{-(p+\lambda)t}}{\pi} \int_0^t \frac{e^{-z^2/(4\alpha_z \tau)}}{\sqrt{\tau(t-\tau)}} u(1-t+\tau)d\tau \tag{A15}$$

Applying the convolution theorem to (A12) and (A15), we obtain

$$\mathcal{L}_s^{-1}\left\{\frac{e^{-z\sqrt{(s+p+\lambda)/\alpha_z}}}{s} erf(\sqrt{s+p+\lambda})\right\} = \frac{e^{-(p+\lambda)t}}{\pi} \int_0^t \frac{e^{-z^2/(4\alpha_z \tau)}}{\sqrt{\tau(t-\tau)}} u(1-t+\tau)d\tau +$$

$$\frac{1}{\pi} \int_0^t (p+\lambda) e^{-(p+\lambda)T} dT \int_0^T \frac{e^{-z^2/(4\alpha_z \tau)}}{\sqrt{\tau(T-\tau)}} u(1-T+\tau)d\tau \tag{A16}$$

Applying (A1C) and (A1D), we obtain

$$\mathcal{L}_p^{-1}\{\mathcal{L}_s^{-1}\{g_3\}\} = \frac{1}{\pi}e^{-\lambda t}u(x+1-t)\int_0^t \frac{e^{-z^2/(4\alpha_z\tau)}}{\sqrt{\tau(t-\tau)}}u(1-t+\tau)d\tau +$$

$$\frac{1}{\pi}\int_0^t [\delta(x+1-T)+\lambda u(x+1-T)]e^{-\lambda T}dT\int_0^T \frac{e^{-z^2/(4\alpha_z\tau)}}{\sqrt{\tau(T-\tau)}}u(1-T+\tau)d\tau \qquad \text{(A17)}$$

In a similar way we can also obtain the inversion for (25D)

$$\mathcal{L}_p^{-1}\{\mathcal{L}_s^{-1}\{g_4\}\} = \frac{1}{\pi}e^{-\lambda t}\int_0^t \frac{e^{-z^2/(4\alpha_z\tau)}}{\sqrt{\tau(t-\tau)}}u(1-t+\tau)u(x-\tau)d\tau +$$

$$\frac{\lambda}{\pi}\int_0^t e^{-\lambda T}dT\int_0^T \frac{e^{-z^2/(4\alpha_z\tau)}}{\sqrt{\tau(T-\tau)}}u(1-T+\tau)u(x-\tau)d\tau \qquad \text{(A18)}$$

Analyses for three different cases based on the definitions of the Heaviside unit function and the Dirac δ function lead to the final solution of (26A) through (26C). In fact, we can prove that the solutions in two different regions give the same result at the interface, $x=0$, using the following identity (Gradshteyn and Ryzhik, 1965. pp. 315)

$$\int_u^\infty \frac{e^{-ay}}{y\sqrt{y-u}}dy = \frac{\pi}{\sqrt{u}}erfc(\sqrt{au}) \qquad \text{(A19)}$$

Derivation of (43A) and (43B)

Taking a finite element, dx' along the NAPL source, we can write

$$dM_z' = -v'\alpha_z'\left(\frac{\partial C_1'}{\partial z'}\right)_{z'=0}dx' \qquad \text{(A20A)}$$

which can be easily converted to the dimensionless equation

$$dM_z = -\left(\frac{\partial C_1}{\partial z}\right)_{z=0} dx \qquad \text{(A20B)}$$

by using Equations (2), (3) and (44).

Substituting (18A) and (18B) into (A20B), and integrating it from -1 to 0, we obtain

$$M_z = \frac{1}{\sqrt{\pi\,\alpha_z}} \int_{-1}^{0} \frac{dx}{\sqrt{T}} \qquad \text{(A21)}$$

where

$$T = t \qquad (t \le x+1) \qquad \text{(A22A)}$$

$$T = x + 1 \qquad (t \ge x+1) \qquad \text{(A22B)}$$

For the case of $t<1$, we can rewrite (22A) and (22B) as

$$T = t \qquad (t-1 \le x \le 0) \qquad \text{(A23A)}$$

$$T = x + 1 \qquad (-1 \le x \le t-1) \qquad \text{(A23B)}$$

For the case of $t>1$, noting that $x<0$, we simply have

$$T \equiv x + 1 \qquad (-1 \le x \le 0) \qquad \text{(A24)}$$

For the two different cases, if we substitute the expressions for T to (A21), and integrate the resulting equation, we obtain solution (43A) and (43B).

Derivation of (45A) and (45B)

Taking a finite element, dz' along $x=0$, we can write

$$dM_x' = v' C_1'(0,z',t')\,dz' \qquad \text{(A25A)}$$

which can be easily converted to the dimensionless equation

$$dM_x = \frac{C_1(0,z,t)\,dz}{\alpha_z} \tag{A25B}$$

by using Equations (2), (3) and (46).

Substituting (18A) and (18B) into (A25B), and integrating it from 0 to ∞, we obtain (45A) and (45B) by using the following formula (Gradshteyn and Ryzhik, 1980)

$$\int_0^\infty erfc(px)\,x^{2q-1}\,dx = \frac{\Gamma(q+1/2)}{2\sqrt{\pi}\,q\,p^{2q}} \tag{A26}$$

and the fact, $\Gamma(1)=1$.

List of Figures

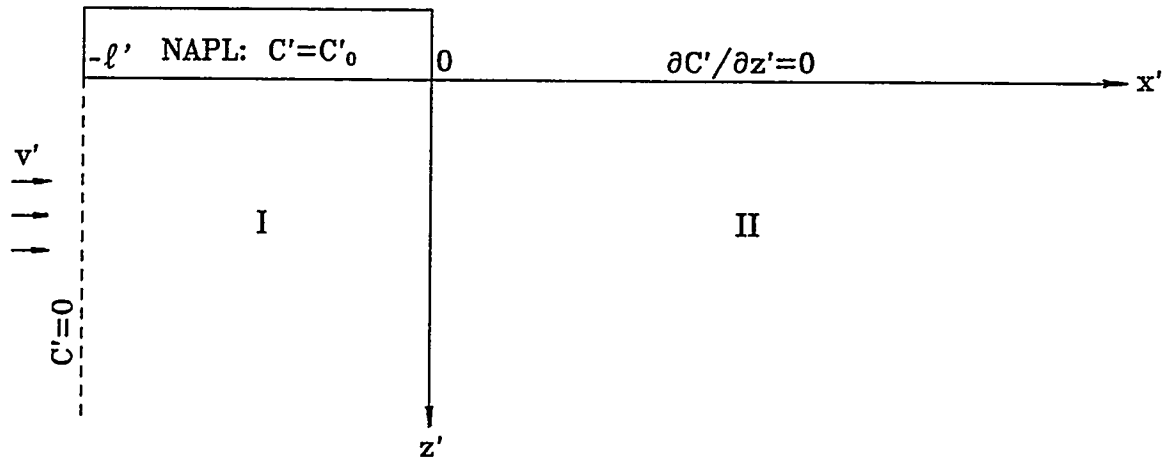

Figure 1. A schematic diagram of the mathematical model

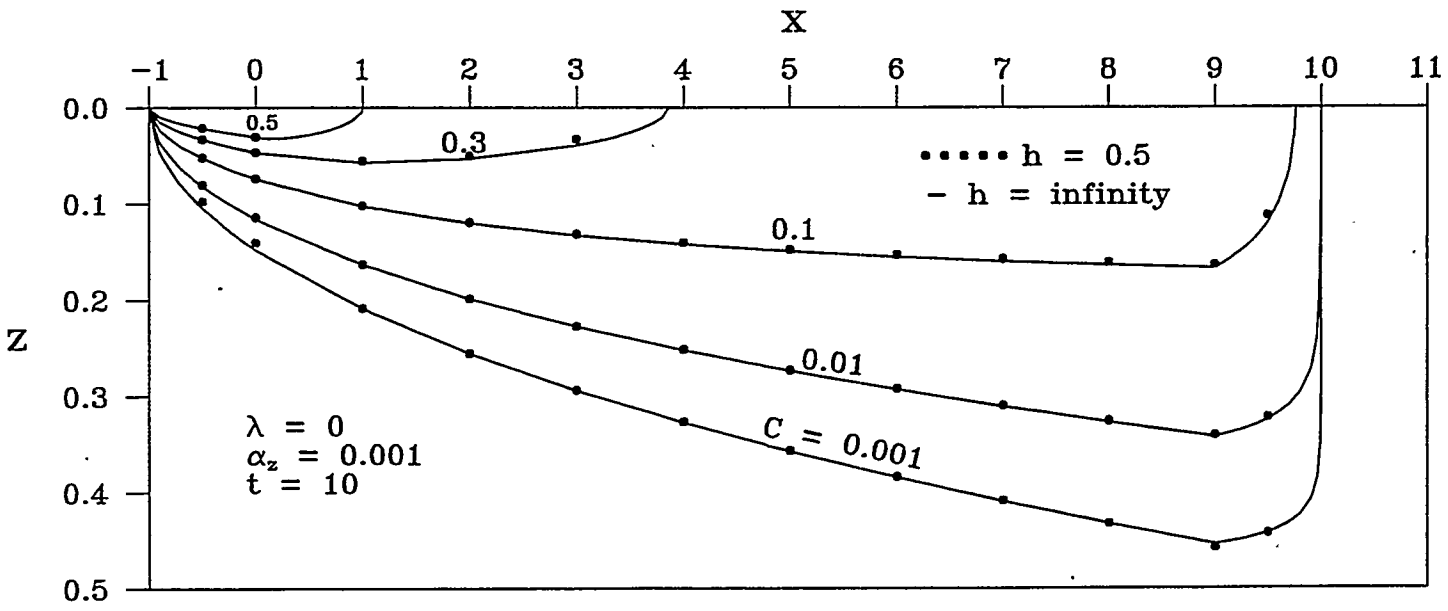

Figure 2. Comparison of two solutions

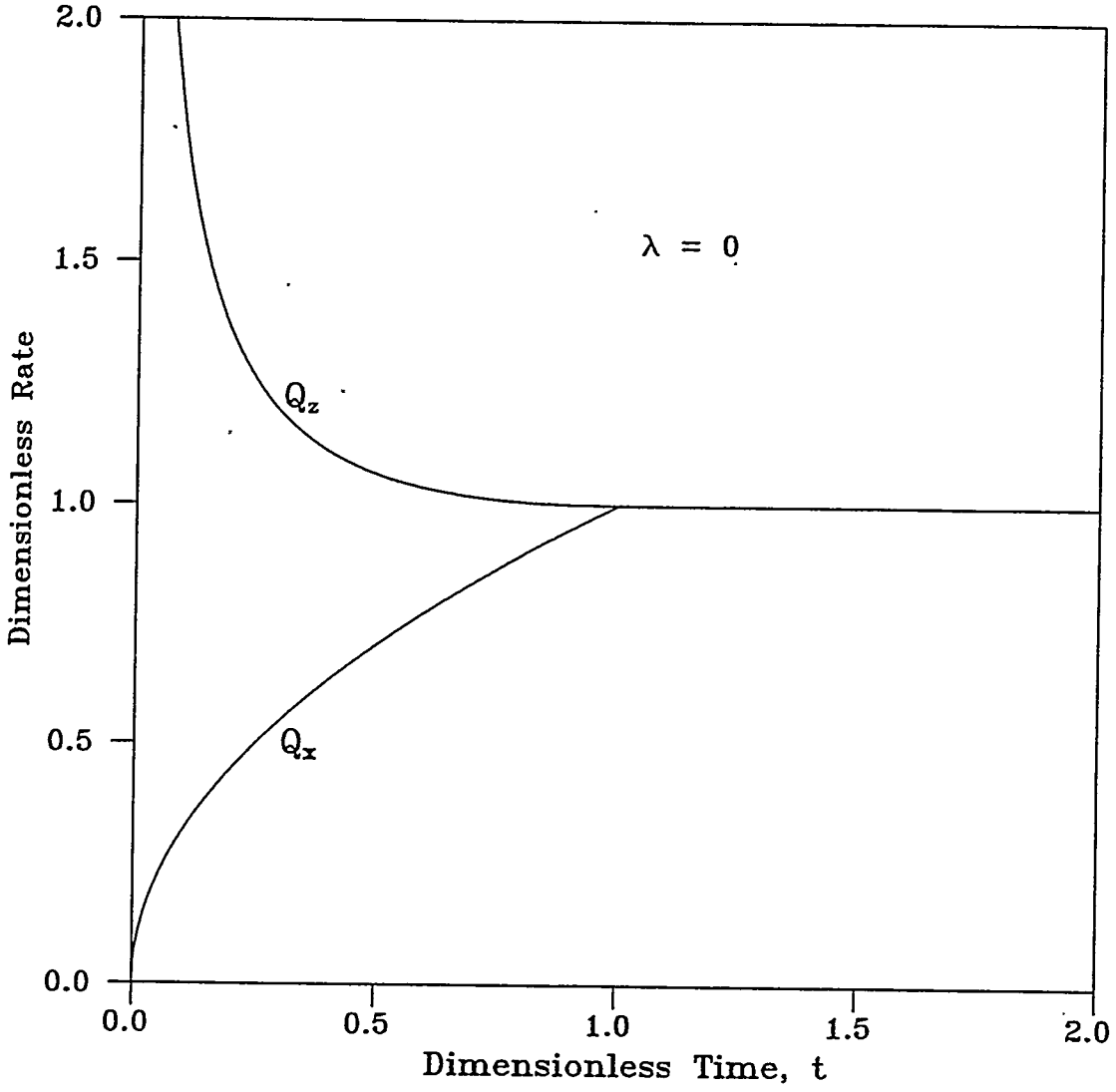

Figure 3. Variation of vertical and horizontal mass transfer rates

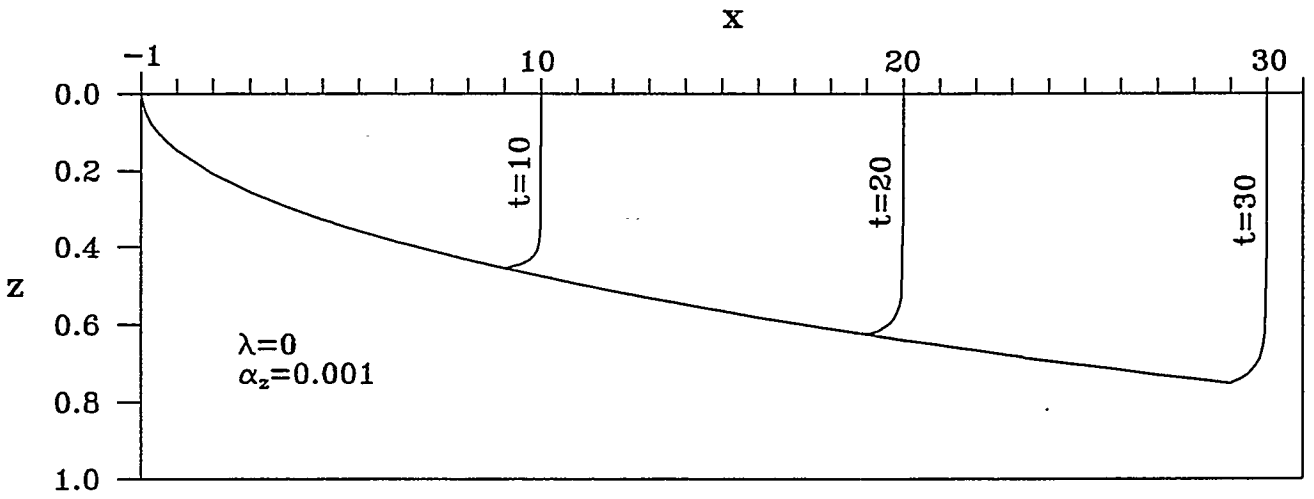

Figure 4. Contamination front (C=0.001) movement

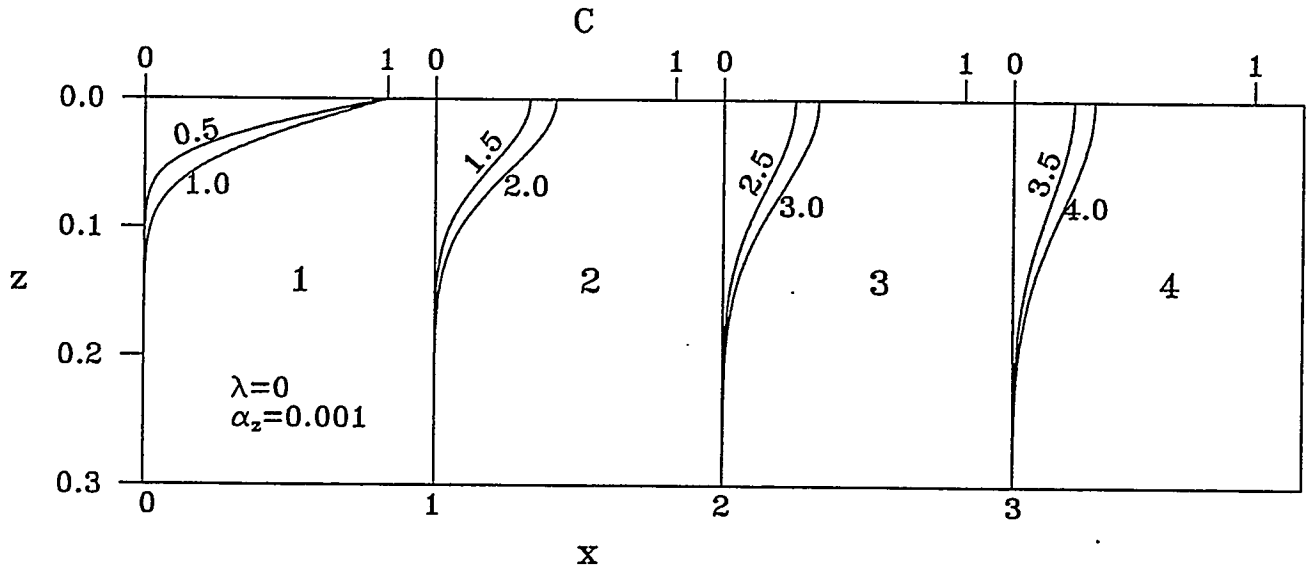

Figure 5. Relative concentration profiles at x = 0, 1, 2, 3

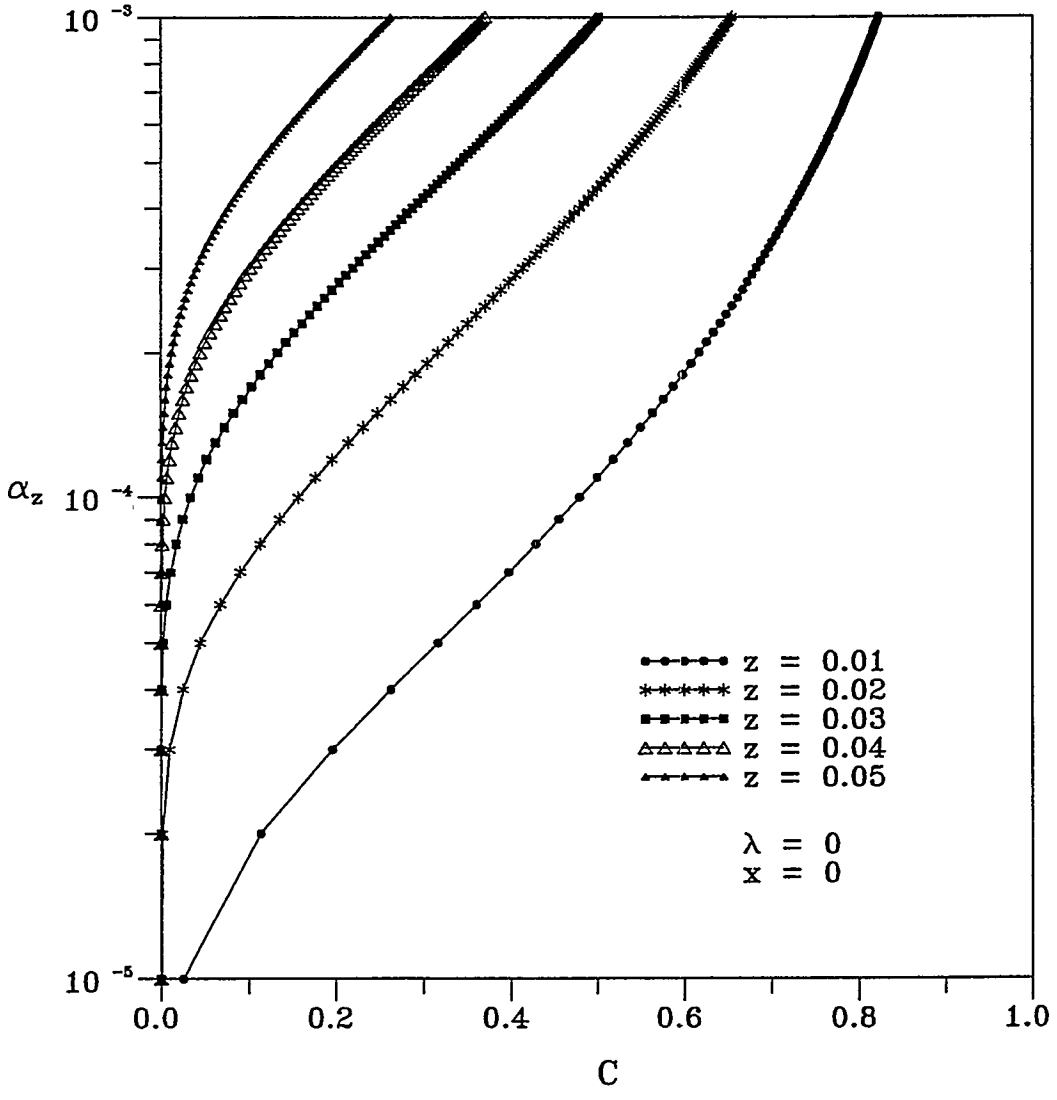

Figure 6. Steady relative concentration as a function of vertical dispersivity

Part 2.

Exact Solutions for Sources with Constant Flux Rate

Two-Dimensional Analytical Solutions for Chemical Transport in Aquifers: 2. Exact Solutions for Sources with Constant Flux Rate

CHAO SHAN AND IRAJ JAVANDEL

Earth Sciences Division, Lawrence Berkeley National Laboratory

University of California, Berkeley

Berkeley, CA 94720, USA

In part 1 of the series [*Shan and Javandel*, the same issue], analytical solutions are developed for the dissolution and transport of nonaqueous phase liquids in a vertical section of a homogeneous aquifer. The source condition used in part 1 is a constant concentration of known value. In part 2, we will present analytical solutions for cases in which a constant flux source is located on the top of an aquifer with a uniformly horizontal flow. The solutions consider advection in the horizontal direction, dispersion in both the horizontal and vertical directions, linear adsorption, and biodegradation. Example calculations are given to show the contamination contours, the effect of degradation, the effect of horizontal and vertical dispersivities, and an application of the solution to determine the two dispersivities. The analytical solutions can be useful in designing an appropriate monitoring and remedial system for handling hazardous leachate from a landfill.

INTRODUCTION

In part 1 of this series [*Shan and Javandel*, 1996] approximate analytical solutions have been given to calculate the transport of a dissolved nonaqueous phase liquid (NAPL) in a vertical section (along the groundwater flow direction) of a homogeneous aquifer. Depending on the density contrast with water, the NAPL source could be located either on the top or at the bottom of the aquifer. In one solution, the finite thickness of the aquifer is considered; while the other solution assumes a semi-infinite thickness for the aquifer. Both solutions were derived for the case of a constant source concentration. In practice, there is another kind of possible source condition, i.e., where the mass flux rate is a constant of known value. A typical example for this case is the groundwater contamination in an unconfined aquifer that receives leachate from the vadose zone.

The transport of leachate in an unconfined aquifer has been studied by several researchers. *Huyakorn et al.* (1987) presented an analytical model for predicting contaminant transport from a Gaussian vertical strip source in a uniform groundwater flow field. In their study, the effect of partial penetration of the contamination source and a finite aquifer thickness were considered. The source is on a plane perpendicular to the direction of groundwater flow. *Ostendorf et al.* (1984) modeled the transport of a simply reactive contaminant through a landfill and an initially clean unconfined aquifer that has a sloping bottom. An analytical solution was derived for the case of a constant mass loading rate into a steady uniform aquifer flow. In deriving the solution, they assumed a first-order reaction kinetics and the absence of dispersion and downgradient dilution. The solution is actually one-dimensional from the transport point of view. Five years later, *Ostendorf et al.* (1989) presented another solution for the leachate transport. They modeled the two-dimensional transport of a nonreactive constituent in an unconfined aquifer with a gently sloping bottom. The two-dimensional flow field in a vertical section was first calculated using the existing analytical solutions [*Gelhar and Wilson*, 1974; *Ostendorf et al.*, 1984]. The results were then used for the transport calculation using some existing analytical solutions [*Ogata*

and Banks, 1961; *Parker and van Genuchten*, 1984]. In summary, they calculated the transport process by using the analytical solution for the vertical advection-dispersion equation on a moving reference frame. The problem was also studied by *Chrysikopoulos et al.* [1994] through comparing the results of a laboratory experiment with an analytical solution for aquifers of infinite thickness. Due to the effect of the impermeable lower boundary in their experiment, the measured concentration is larger than the calculated concentration at later times. In part 2 of this series, we want to solve the two-dimensional advection-dispersion equation using a constant flux source of finite length on top of the aquifer. Analytical solutions will be derived for aquifers with finite thickness or assumed infinite thickness. Discussions will be given on the effects of decay, the horizontal and vertical dispersivities, as well as to the potential application of the analytical solutions in determining the dispersivities.

THEORY

The study in part 2 is based on the following assumptions: (1) the aquifer is homogeneous and has a uniform thickness, h'; (2) the constant infiltration rate, q' is so small that flow in the aquifer is in the horizontal direction with an average pore velocity, v'; (3) the concentration of the leachate is a constant, C_0'; and (4) the source has such a large width that the sectional model is valid. We choose the x' axis at the water table in the groundwater flow direction, the z' axis vertically downwards, and the origin at the down-gradient end of the source (Figure 1). The whole aquifer is divided into three regions by the z' axis and the line, $x'=-\ell'$: Region 1 ($-\ell' \le x' \le 0$), Region 2 ($0 \le x' < +\infty$), and Region 3 ($-\infty < x' \le -\ell'$) where ℓ' is the length of the source in the flow direction. The dimensionless governing equations for all three regions, however, can be written in a unified form:

$$\frac{\partial C_n}{\partial t} + \lambda C_n + \frac{\partial C_n}{\partial x} - \alpha_x \frac{\partial^2 C_n}{\partial x^2} - \alpha_z \frac{\partial^2 C_n}{\partial z^2} = 0 \qquad (n=1,2,3) \tag{1}$$

where the dimensional variables and parameters are defined by

$$C_n = C'_n / C'_0 \tag{2}$$

$$x = \frac{x'}{\ell'}, \qquad z = \frac{z'}{\ell'}, \qquad h = \frac{h'}{\ell'}, \qquad t = \frac{v' t'}{R' \ell'} \tag{3}$$

$$\alpha_x = \frac{\alpha'_x}{\ell'}, \qquad \alpha_z = \frac{\alpha'_z}{\ell'}, \qquad q = \frac{q'}{v'}, \qquad \lambda = \frac{R' \ell' \lambda'}{v'} \tag{4}$$

where C'_n ($n=1,2,3$) represent the chemical concentration in Regions 1, 2, and 3, respectively; t' is time; λ' is the decay constant; R' is the retardation factor; α'_x and α'_z are the "apparent dispersivities" in the horizontal and vertical directions, respectively, which represent the combined effect of hydrodynamic dispersion and molecular diffusion.

The dimensionless initial and boundary conditions for the problem are

$$C_n(x,z,0) = 0 \tag{5}$$

$$\frac{\partial C_1(x,0,t)}{\partial z} = -\frac{q}{\alpha_z} \tag{6}$$

$$\frac{\partial C_i(x,0,t)}{\partial z} = 0 \qquad (i=2,3) \tag{7}$$

$$C_2(\infty,z,t) = 0 \tag{8}$$

$$C_3(-\infty,z,t) = 0 \tag{9}$$

$$C_1(0,z,t) = C_2(0,z,t) \tag{10a}$$

$$\frac{\partial C_1(0,z,t)}{\partial x} = \frac{\partial C_2(0,z,t)}{\partial x} \tag{10b}$$

$$C_1(-1,z,t) = C_3(-1,z,t) \tag{11a}$$

$$\frac{\partial C_1(-1,z,t)}{\partial x} = \frac{\partial C_3(-1,z,t)}{\partial x} \tag{11b}$$

The boundary condition at the bottom of the aquifer ($z'=h'$) has not been given because we want to derive the solutions for two different cases.

Case 1. Infinite h'

For this case, we assume that h' is so large that the contaminant front will not reach the bottom of the aquifer within the time of calculation. Based on this assumption, we may use the following boundary condition:

$$C_n(x,\infty,t) = 0 \tag{12}$$

We now solve (1) under the above initial and boundary conditions.

Applying the Laplace transform with respect to t and the Fourier cosine transform with respect to z, consecutively, (1) is reduced to the form

$$\alpha_x \frac{d^2 C_{nLF}}{dx^2} - \frac{dC_{nLF}}{dx} - (s+\lambda+\alpha_z r^2) C_{nLF} = f_n \tag{13a}$$

where

$$f_1 = -q/s\ , \qquad f_2 = f_3 = 0 \tag{13b}$$

where s and r are the Laplace and Fourier cosine transform parameters, respectively; and C_{nLF} is defined by

$$C_{nLF}(x,r,s) = \int_0^\infty C_{nL}(x,z,s)\cos(rz)\,dz \tag{14}$$

$$C_{nL}(x,z,s) = \int_0^\infty C_n(x,z,t)e^{-st}\,dt \tag{15}$$

The solutions of (13) which can satisfy the boundary conditions (8) through (11) in the transformed domain are

$$C_{1LF} = \frac{-2\alpha_x q}{As(A+1)} e^{(A+1)x/(2\alpha_x)} - \frac{2\alpha_x q}{As(A-1)} e^{(1-A)(x+1)/(2\alpha_x)} + \frac{4\alpha_x q}{s(A^2-1)} \tag{16a}$$

$$C_{2LF} = \frac{2\alpha_x q}{As(A-1)}\left[e^{(1-A)x/(2\alpha_x)} - e^{(1-A)(x+1)/(2\alpha_x)}\right] \tag{16b}$$

$$C_{3LF} = \frac{2\alpha_x q}{As(A+1)}\left[e^{(A+1)(x+1)/(2\alpha_x)} - e^{(A+1)x/(2\alpha_x)}\right] \tag{16c}$$

where

$$A = \sqrt{4\alpha_x(s + \lambda + \alpha_z r^2) + 1} \tag{17}$$

For Equation (16), if we take the inverse Laplace transform with respect to s and the inverse Fourier cosine transform with respect to r, consecutively, we obtain (a detailed derivation process is given in Appendix A)

$$C_1 = \frac{q}{2\sqrt{\lambda\alpha_z}}\left[e^{-z\sqrt{\lambda/\alpha_z}}erfc\left(\frac{z}{2\sqrt{\alpha_z t}} - \sqrt{\lambda t}\right) - e^{z\sqrt{\lambda/\alpha_z}}erfc\left(\frac{z}{2\sqrt{\alpha_z t}} + \sqrt{\lambda t}\right)\right] -$$

$$\frac{q}{2\sqrt{\pi\alpha_z}}\int_0^t e^{-z^2/(4\alpha_z\tau)-\lambda\tau}\left[erfc\left(\frac{\tau - x}{2\sqrt{\alpha_x\tau}}\right) + erfc\left(\frac{x+1-\tau}{2\sqrt{\alpha_x\tau}}\right)\right]\frac{d\tau}{\sqrt{\tau}} \tag{18a}$$

$$C_2 = \frac{q}{2\sqrt{\pi\alpha_z}}\int_0^t e^{-z^2/(4\alpha_z\tau)-\lambda\tau}\left[erfc\left(\frac{x - \tau}{2\sqrt{\alpha_x\tau}}\right) - erfc\left(\frac{x+1-\tau}{2\sqrt{\alpha_x\tau}}\right)\right]\frac{d\tau}{\sqrt{\tau}} \tag{18b}$$

$$C_3 = \frac{q}{2\sqrt{\pi\alpha_z}}\int_0^t e^{-z^2/(4\alpha_z\tau)-\lambda\tau}\left[erfc\left(\frac{\tau - x - 1}{2\sqrt{\alpha_x\tau}}\right) - erfc\left(\frac{\tau - x}{2\sqrt{\alpha_x\tau}}\right)\right]\frac{d\tau}{\sqrt{\tau}} \tag{18c}$$

For some cases, we may not want to consider the decay effect such that $\lambda=0$. Under this circumstance, the first term in (18a) should be replaced by the inversion given in (A6).

Case 2. Finite h'

For this case, the lower boundary condition, (12) needs to be replaced by

$$\frac{\partial C_n(x,h,t)}{\partial z} = 0 \tag{19}$$

The solution procedure is almost the same as that for the infinite h' case, except that we need to apply the finite Fourier cosine transform (*Churchill*, 1958)

$$C_{nLf}(x,m,s) = \int_0^h C_{nL}(x,z,s)\cos(b_m z)\,dz \tag{20}$$

where C_{nL} is defined by (15), and b_m is defined by

$$b_m = \frac{m\pi}{h} \tag{21}$$

Apparently, the equations in the transformed domain are exactly the same as (13a) except that the subscripts, F and the parameter r should be replaced by f and b_m, respectively. The definition for f_n is still given by (13b). In addition, the boundary conditions in the transformed domain are exactly the same as those for the infinite h' case. As a result, the solutions in the transformed domain for three regions are exactly the same as (16a) through (16c), except that F should be replaced by f. Correspondingly, r should be replaced by b_m.

The inversion procedure is also similar to that for (16a) through (16c), which has been shown in Appendix A. The only difference is that after the Laplace inversion, we need to apply the inversion formula for the finite Fourier cosine transform (*Churchill*, 1958)

$$C_n(x,z,t) = \frac{1}{h}C_{nf}(x,0,t) + \frac{2}{h}\sum_{m=1}^{\infty} C_{nf}(x,m,t)\cos(b_m z) \tag{22}$$

The final solutions for the three regions are

$$C_1 = \frac{q(1-e^{-\lambda t})}{\lambda h} + \frac{2q}{h}\sum_{m=1}^{\infty}\frac{1-e^{-(\lambda+\alpha_z b_m^2)t}}{\lambda+\alpha_z b_m^2}\cos(b_m z) -$$

$$\frac{q}{2h}\int_0^t e^{-\lambda\tau}\left[erfc\left(\frac{\tau-x}{2\sqrt{\alpha_x\tau}}\right)+erfc\left(\frac{x+1-\tau}{2\sqrt{\alpha_x\tau}}\right)\right]d\tau -$$

$$\frac{q}{h}\sum_{m=1}^{\infty}\cos(b_m z)\int_0^t e^{-\alpha_z b_m^2\tau-\lambda\tau}\left[erfc\left(\frac{\tau-x}{2\sqrt{\alpha_x\tau}}\right)+erfc\left(\frac{x+1-\tau}{2\sqrt{\alpha_x\tau}}\right)\right]d\tau \tag{23a}$$

$$C_2 = \frac{q}{2h}\int_0^t e^{-\lambda\tau}\left[erfc\left(\frac{x-\tau}{2\sqrt{\alpha_x\tau}}\right) - erfc\left(\frac{x+1-\tau}{2\sqrt{\alpha_x\tau}}\right)\right]d\tau +$$

$$\frac{q}{h}\sum_{m=1}^{\infty}\cos(b_m z)\int_0^t e^{-\alpha_z b_m^2\tau-\lambda\tau}\left[erfc\left(\frac{x-\tau}{2\sqrt{\alpha_x\tau}}\right) - erfc\left(\frac{x+1-\tau}{2\sqrt{\alpha_x\tau}}\right)\right]d\tau \qquad (23b)$$

$$C_3 = \frac{q}{2h}\int_0^t e^{-\lambda\tau}\left[erfc\left(\frac{\tau-x-1}{2\sqrt{\alpha_x\tau}}\right) - erfc\left(\frac{\tau-x}{2\sqrt{\alpha_x\tau}}\right)\right]d\tau +$$

$$\frac{q}{h}\sum_{m=1}^{\infty}\cos(b_m z)\int_0^t e^{-\alpha_z b_m^2\tau-\lambda\tau}\left[erfc\left(\frac{\tau-x-1}{2\sqrt{\alpha_x\tau}}\right) - erfc\left(\frac{\tau-x}{2\sqrt{\alpha_x\tau}}\right)\right]d\tau \qquad (23c)$$

For the case of $\lambda=0$, the first term in (23a) can be reduced to qt/h by applying the L'Hospital rule.

RESULTS AND APPLICATIONS

The two analytical solutions for the two cases (infinite and finite thickness, h) are compared in Figure 2, where the solid curves are calculated form the infinite thickness solution, and the dots are calculated from the finite thickness solution using a dimensionless thickness, $h=0.5$. The agreement between the two solutions is excellent. The other parameters used to obtain Figure 2 are $\lambda=0$, $\alpha_x=0.1$, $\alpha_z=0.001$, $q=0.1$ and $t=10$. This figure indicates that the analytical solution for the case of infinite aquifer thickness is applicable to practical problems if (a) the aquifer has a relatively large thickness, or (b) the contamination front has not reached the bottom of the aquifer at the calculation time. In cases where the contamination front has reached the bottom of the aquifer at the calculation time (probably due to a small aquifer thickness, a large vertical dispersivity, and a large calculation time), one needs to apply

the analytical solution for aquifers with finite thickness. There are several points to be remembered in the application of the finite thickness solution: (a) the solution cannot be used to calculate the concentrations exactly at $z=0$ and $z=h$, (b) when the calculation is performed for points close to the upper and lower boundaries and points in region 1, more terms should be taken from the infinite series in order to achieve a high accuracy. For example, the data points in Figure 2 were obtained by taking 50 terms for points in regions 2 and 3, and 200 terms for points in region 1 ($x=-0.5$). Since the solution for the infinite thickness case is simple and applicable in most cases, we will use it in the following calculations.

Contamination Front Movement

In many cases, people are concerned about how the contamination front moves through the aquifer, particularly, how the front develops downwards. As an example, we take the relative concentration contour, $C=0.01$ as the contamination front in the following studies. For $\lambda=0$, $\alpha_x=0.1$, $\alpha_z=0.001$ and $q=0.1$, the contamination fronts at three different times, $t=1$, 5, and 10 are shown in Figure 3. This figure implies that sooner or later, the contamination front at certain distance downgradient will reach a maximum depth and become stable. The maximum depth increases in the groundwater flow direction. This figure can be useful in determining the depth of a monitoring or remediation well.

Decay Effect

We can apply the solution to study the effect of decay. The dimensionless decay constant, λ is defined as the product of the decay constant, λ', the retardation factor, R', and the length of the source, ℓ' divided by the average linear groundwater velocity, v' (see definition equation 4). Depending on different chemicals in different problems, the dimensionless decay constant, λ can be zero or large positive values. For convenience, we take $\lambda=0$, 0.1, 0.5, and 1 to show the effect of decay. Using $\alpha_x=0.1$, $\alpha_z=0.001$ and $q=0.1$, the contamination fronts ($C=0.01$) corresponding to the four different

λ values at $t=10$ are shown in Figure 4. Apparently, the contamination in the aquifer can be significantly reduced as λ increases from 0 to 1.

Effect of Horizontal Dispersivity

The effect of α_x is shown in Figure 5, where $\lambda=0$, $\alpha_z=0.001$, and $q=0.1$ have been used. The three curves in Figure 5 represent the contamination fronts at $t=10$ for three different α_x values. As α_x increases, more front spreading is observed in both the up-gradient and down-gradient directions. One can also find that as α_x becomes very small, the contamination front is very sharp at the down-gradient end, and the shape of the curve (corresponding to $\alpha_x=0.01$ in Figure 5) is very similar to what we have obtained in the part 1 of this series [*Shan and Javandel*, 1996], where we have neglected horizontal dispersion.

Effect of Vertical Dispersivity

Similarly, the effect of α_z can be shown by varying its value and fixing other parameters. Using $\lambda=0$, $\alpha_x=0.1$, $q=0.1$ and $t=10$, the contamination front ($C=0.01$) for $\alpha_z=0.01$, 0.001, and 0.0001 were calculated and shown in Figure 6. As it is expected, a larger vertical dispersivity, α_z always causes a larger dispersion in the vertical direction and a smaller dispersion in the horizontal direction.

Method to Determine Dispersivities

Methods for determining dispersivities have been investigated by many researchers [e.g., *Robbins*, 1989; *Syriopoulou and Koussis*, 1991]. In the above calculations, we have assumed that the two dispersivities are some known values. The solutions, however, can also be applied inversely to determine the dispersivities in a tracer test. To improve the test efficiency, samples need to be collected at favorable locations. It is recommended that wells be drilled at a short distance down-gradient from the source and screened close to the top of the aquifer. There are three advantages in doing so: (1) the concentrations

are relatively high and the measurement error can be relatively small; (2) it takes less time to obtain data, particularly steady state measurements; and (3) there is a better chance to obtain samples with measurable concentrations. Following this kind of optimal design, we can apply the simplified solution at region 2 (set $z=0$ in equation 18b) to determine the dispersivities. In the following, we will assume $\lambda=0$ for convenience. By substituting $z=0$ and $\lambda=0$ into (18b), we obtain

$$C = \frac{qI}{2\sqrt{\pi\alpha_z}} \tag{24a}$$

where

$$I = \int_0^t \left[erfc\left(\frac{x-\tau}{2\sqrt{\alpha_x\tau}}\right) - erfc\left(\frac{x+1-\tau}{2\sqrt{\alpha_x\tau}}\right)\right]\frac{d\tau}{\sqrt{\tau}} \tag{24b}$$

In practice, we may want to use the observed steady-state concentration to determine the dispersivities. Correspondingly, we can calculate the steady-state concentration by setting $t=\infty$ in (24b). To obtain both α_x and α_z from the same test, we may need two wells at two different locations: $x=x_A$ and $x=x_B$, and observe the steady-state concentrations, C_A and C_B. Applying (24a), we obtain the concentration ratio

$$C_r = C_A/C_B = I_A/I_B \tag{25}$$

which is a function of α_x only. Using (24b), a C_r-α_x curve can be calculated. Figure 7 gives an example for $x_A=0.5$ and $x_B=1.0$. Using this curve, one can find the α_x value corresponding to the observed steady-state data. For example, if $C_A=1.225$ and $C_B=1.068$, we calculated $C_r=1.147$. In Figure 7 the corresponding horizontal dispersivity is $\alpha_x=5$. Substituting this dispersivity into (24b), one can calculate the integral at any points as t tends to infinity. For example, at point A, the integral is $I_A=1.373$. Finally, if we substitute the values of I_A, C_A and q ($q=0.1$ for this case) into (24a), we obtain $\alpha_z=0.001$ for this example. In some other cases, if α_x is known, we need to have one well only. The direct application of (24a) and (24b) can give the value of α_z.

CONCLUSION

Two analytical solutions have been derived independently for contaminant transport in an unconfined aquifer in a vertical cross section, one assuming an infinite aquifer thickness, the other using a finite aquifer thickness. The solutions were obtained for cases where a constant mass loading rate from the top of the aquifer can be assumed. The analytical solutions account for advection in the horizontal direction (with constant flow rate), dispersions in the horizontal and vertical directions, adsorption, and decay. A comparison between the two solutions indicates that the solution for the case of *infinite aquifer thickness* is valid for most practical problems. The analytical solutions can be used to predict the contaminant transport in aquifers as well as to determine the dispersivities. Therefore, the solutions developed in this study can be useful in designing a field test for site characterization and in selecting an effective system for site monitoring and remediation.

ACKNOWLEDGMENT

This work was supported in part by California Department of Health Services and in part by the Director, Office of Environmental Management, Office of Environmental Restoration of the U.S. Department of Energy under contract DE-AC03-76SF00098. The authors thank D. B. Stephens for his suggestions and C. Doughty and G. Xie for reviewing the manuscript.

REFERENCES

Chrysikopoulos, C. V., E. A. Voudrias, and M. M. Fyrillas, Modeling of contaminant transport resulting from dissolution of nonaqueous phase liquid pools in saturated porous media, *Transport in Porous Media, 16*: 125-145, 1994.

Churchill, R. V., *Operational Mathematics*, 2nd. ed. McGraw-Hill, New York, 1958.

Erdélyi, A., *Tables of Integral Transforms*, McGraw-Hill Book Company, Inc., New York, 1954.

Gelhar, L. W., and J. L. Wilson, Groundwater quality modeling, *Ground Water, 12: 399-408*, 1974.

Huyakorn, P. S., M. J. Ungs, L. A. Mulkey, and E. A. Sudicky, A three-dimensional analytical method for predicting leachate migration, *Ground Water, 25(5): 588-598*, 1987.

Ogata, A., and R. B. Banks, A solution of the differential equation of longitudinal dispersion in porous media, *U.S. Geol. Surv., Prof. Pap. 411-A*, 7 pp., 1961.

Ostendorf, D. W., R. R. Noss, and D. O. Lederer, Landfill leachate migration through shallow unconfined aquifers, *Water Resour. Res., 20(2): 291-296*, 1984.

Ostendorf, D. W., D. A. Reckhow, and D. J. Popielarczyk, Vertical transport processes in unconfined aquifers, *J. Contam. Hydrol., 4: 93-107*, 1989.

Parker, J. C., and M. T. van Genuchten, Flux averaged and volume averaged concentrations in continuum approaches to solute transport, *Water Resour. Res., 20(7): 866-872*, 1984.

Robbins, G. A., Methods for determining transverse dispersion coefficients of porous media in laboratory column experiments, *Water Resour. Res., 25(6): 1249-1258*, 1989.

Shan, C., and I. Javandel, Analytical solutions for solute transport in a vertical aquifer section: 1. Simplified solutions for sources with constant concentration, *Lawrence Berkeley Laboratory Rep. LBL-38825, Part 1*, 1996.

Syriopoulou, D., and A. D. Koussis, Two-dimensional modeling of advection-dominated solute transport in groundwater by the matched artificial dispersivity method, *Water Resour. Res., 27(5): 865-872*, 1991.

APPENDIX A: SOLUTION DERIVATIONS

For $\lambda > 0$, the inversion of the third term in (16a) is

$$\mathcal{F}_c^{-1}\left\{\mathcal{L}^{-1}\left\{\frac{4\alpha_x q}{s(A^2-1)}\right\}\right\} = \frac{q}{2\sqrt{\lambda\alpha_z}}\left[e^{-z\sqrt{\lambda/\alpha_z}}erfc\left(\frac{z}{2\sqrt{\alpha_z t}}-\sqrt{\lambda t}\right)-e^{z\sqrt{\lambda/\alpha_z}}erfc\left(\frac{z}{2\sqrt{\alpha_z t}}+\sqrt{\lambda t}\right)\right] \tag{A1}$$

in which process we have used (17) and the following inversion formulae [*Erdélyi*, 1954]

$$\mathcal{L}^{-1}\left\{\frac{1}{s(s+a)}\right\} = (1-e^{-at})/a \tag{A2}$$

$$\mathcal{F}_c^{-1}\left\{\frac{1}{r^2+a^2}\right\} = \frac{e^{-az}}{a} \tag{A3}$$

$$\mathcal{F}_c^{-1}\left\{\frac{e^{-b^2r^2}}{r^2+a^2}\right\} = \frac{e^{a^2b^2}}{2a}\left[e^{-az}erfc(ab-\frac{z}{2b}) + e^{az}erfc(ab+\frac{z}{2b})\right] \tag{A4}$$

and the identity of the complementary error function

$$2 - erfc(b-a) = erfc(a-b) \tag{A5}$$

For $\lambda = 0$, the inversion of the third term in (16a) is simply

$$\mathcal{L}^{-1}\left\{\mathcal{F}_c^{-1}\left\{\frac{4\alpha_x q}{s(A^2-1)}\right\}\right\} = \frac{q}{\sqrt{\alpha_z}}\left[\frac{2\sqrt{t}}{\sqrt{\pi}}e^{-z^2/(4\alpha_z t)} - \frac{z}{\sqrt{\alpha_z}}erfc\left(\frac{z}{2\sqrt{\alpha_z t}}\right)\right] \tag{A6}$$

which was derived using (17), (A3) and the Laplace inversion formula [*Erdélyi*, 1954]

$$\mathcal{L}^{-1}\left\{\frac{e^{-a\sqrt{s}}}{s\sqrt{s}}\right\} = \frac{2\sqrt{t}}{\sqrt{\pi}}e^{-a^2/(4t)} - a\cdot erfc\left(\frac{a}{2\sqrt{t}}\right) \tag{A7}$$

The forms of other six terms in (16a) through (16c) are the same. In fact, for $a \geq 0$ and $b = \pm 1$, we have

$$\mathcal{F}^{-1}\left\{\mathcal{L}^{-1}\left\{\frac{e^{-aA}}{sA(A+b)}\right\}\right\} = \frac{e^{ab}}{4\alpha_x\sqrt{\pi\alpha_z}}\int_0^t e^{-z^2/(4\alpha_z\tau)-\lambda\tau}\,erfc\left(\frac{a\sqrt{\alpha_x}}{\sqrt{\tau}}+\frac{b\sqrt{\tau}}{2\sqrt{\alpha_x}}\right)\frac{d\tau}{\sqrt{\tau}} \tag{A8}$$

which was derived using (17) and the following formulae

$$\mathcal{L}^{-1}\{\phi(s+a)\} = e^{-at}\mathcal{L}^{-1}\{\phi(s)\} \tag{A9}$$

$$\mathcal{L}^{-1}\left\{\frac{e^{-a\sqrt{s}}}{\sqrt{s}(\sqrt{s}+b)}\right\} = e^{ab+b^2t}\,erfc\left(\frac{a}{2\sqrt{t}}+b\sqrt{t}\right) \tag{A10}$$

$$\mathcal{L}^{-1}\left\{\frac{\phi(s)}{s}\right\} = \int_0^t \mathcal{L}^{-1}\{\phi(s)\}dt \tag{A11}$$

$$\mathcal{F}_c^{-1}\left\{e^{-ar^2}\right\} = \frac{1}{\sqrt{\pi a}}e^{-z^2/(4a)} \tag{A12}$$

Applying (A1) and (A8) to (16a) through (16c), we obtain the solution for the case of $\lambda>0$. Applying (A6) and (A8) to (16a) through (16c), and setting $\lambda=0$, we obtain the solution for the case of $\lambda=0$.

List of Figures

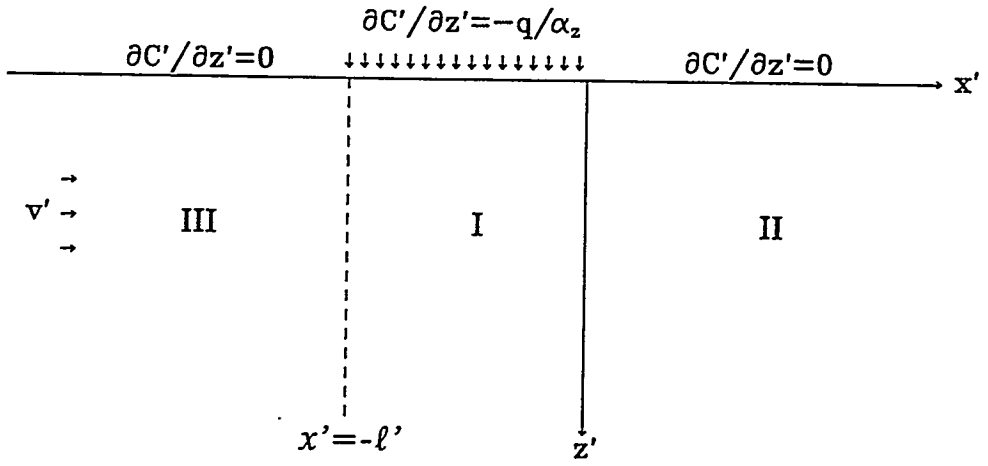

Figure 1. A schematic diagram of the mathematical model

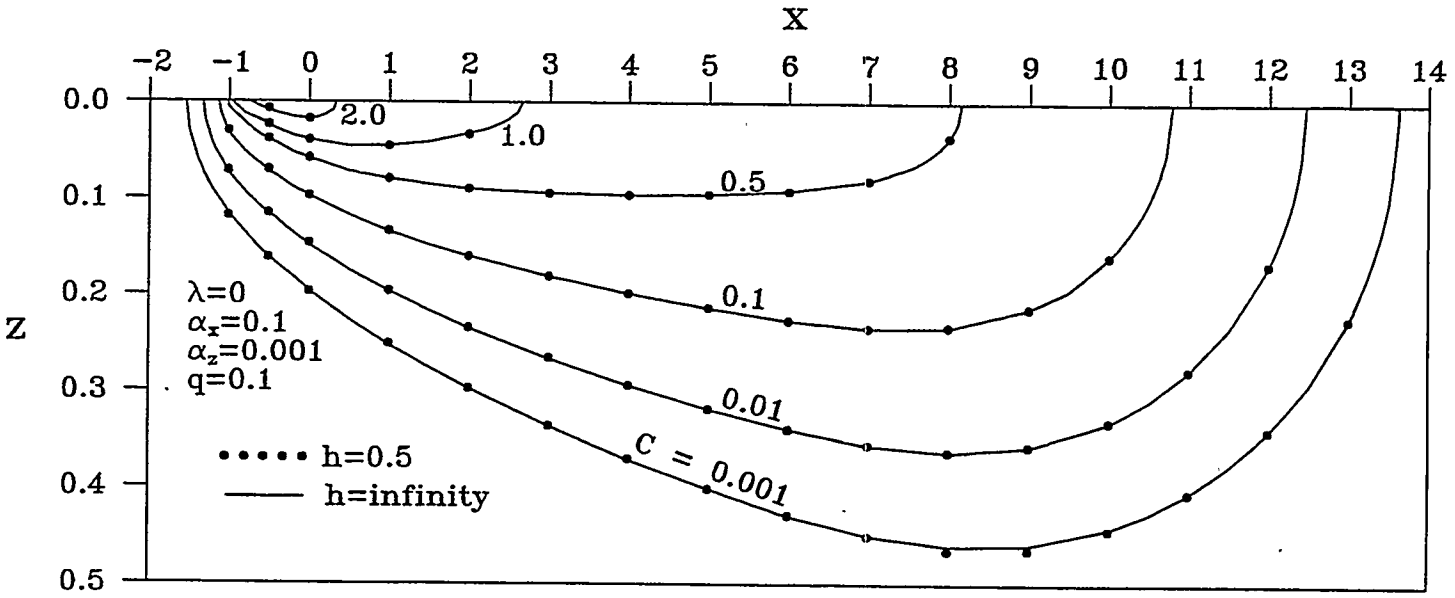

Figure 2. Comparison of relative concentrations at t=10 between two solutions

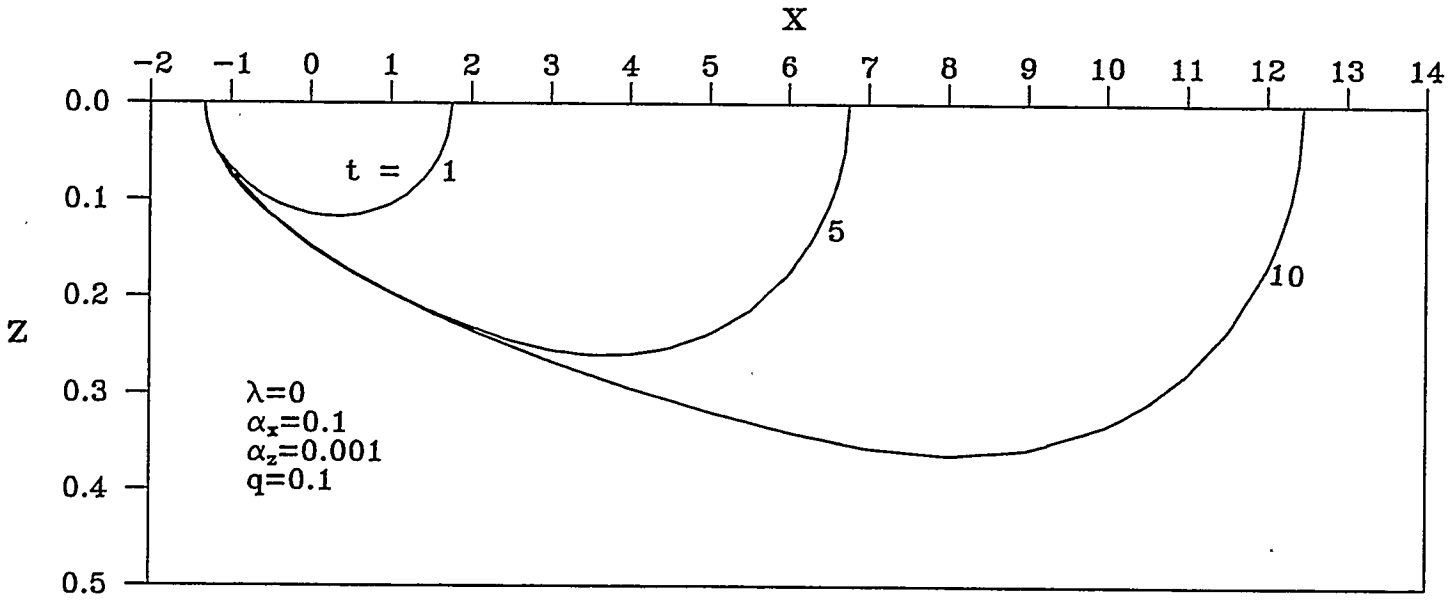

Figure 3. Contamination front (C=0.01) movement

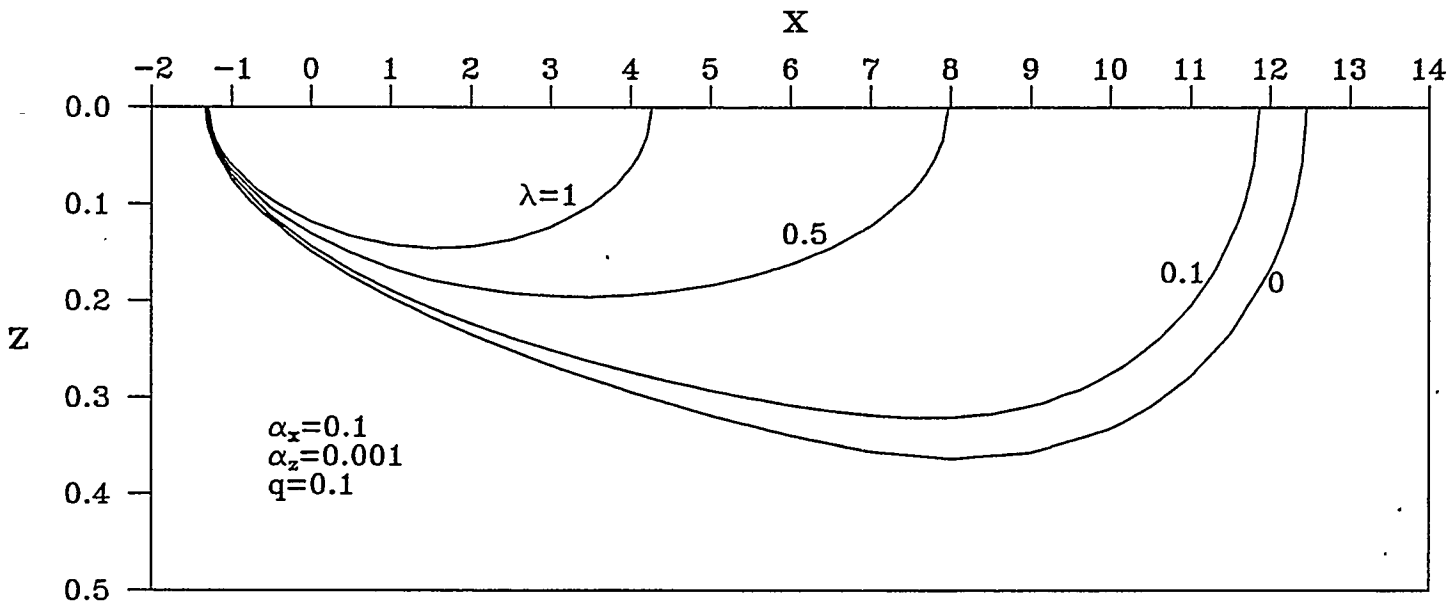

Figure 4. Contamination front (C=0.01) at t=10 for four different λ values

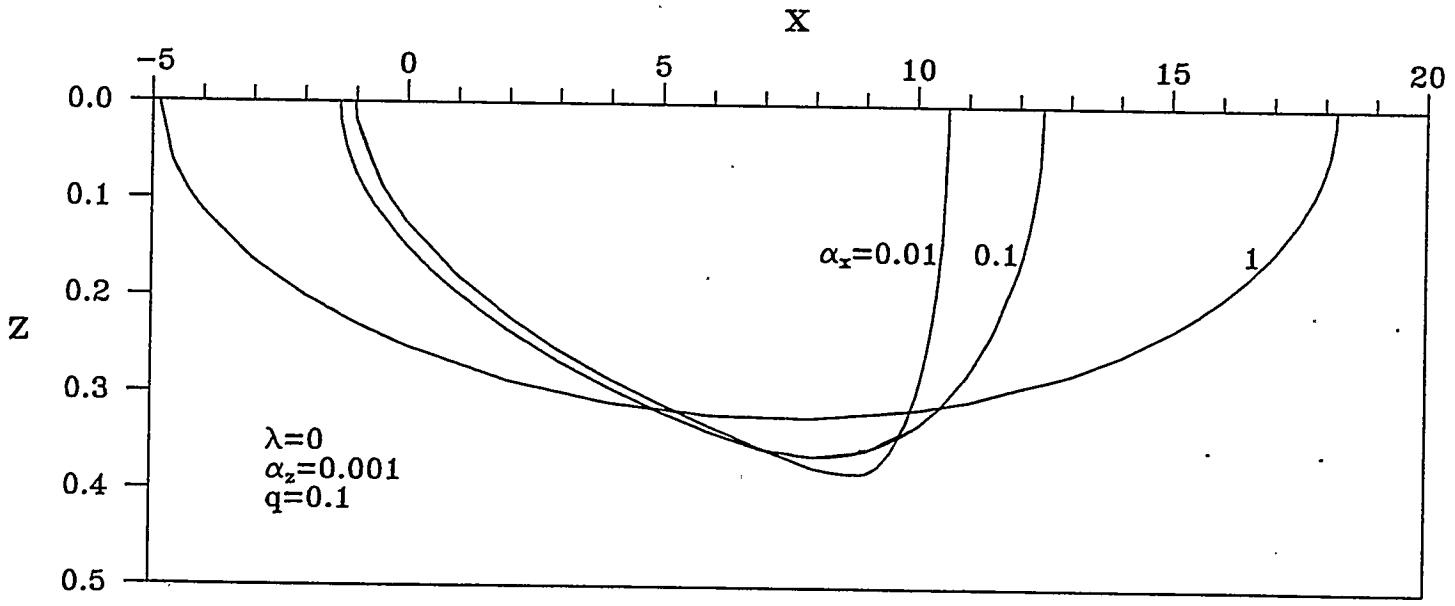

Figure 5. Contamination front (C=0.01) at t=10 for three different α_x values

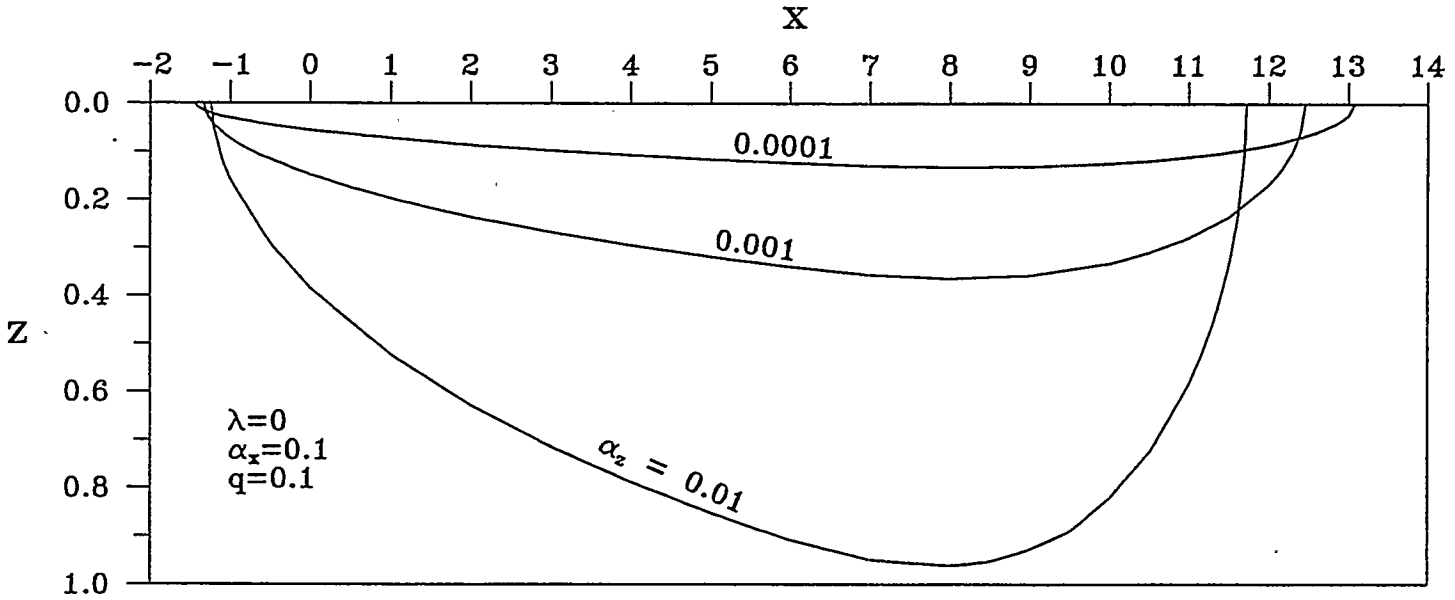

Figure 6. Contamination front (C=0.01) at t=10 for three different α_z values

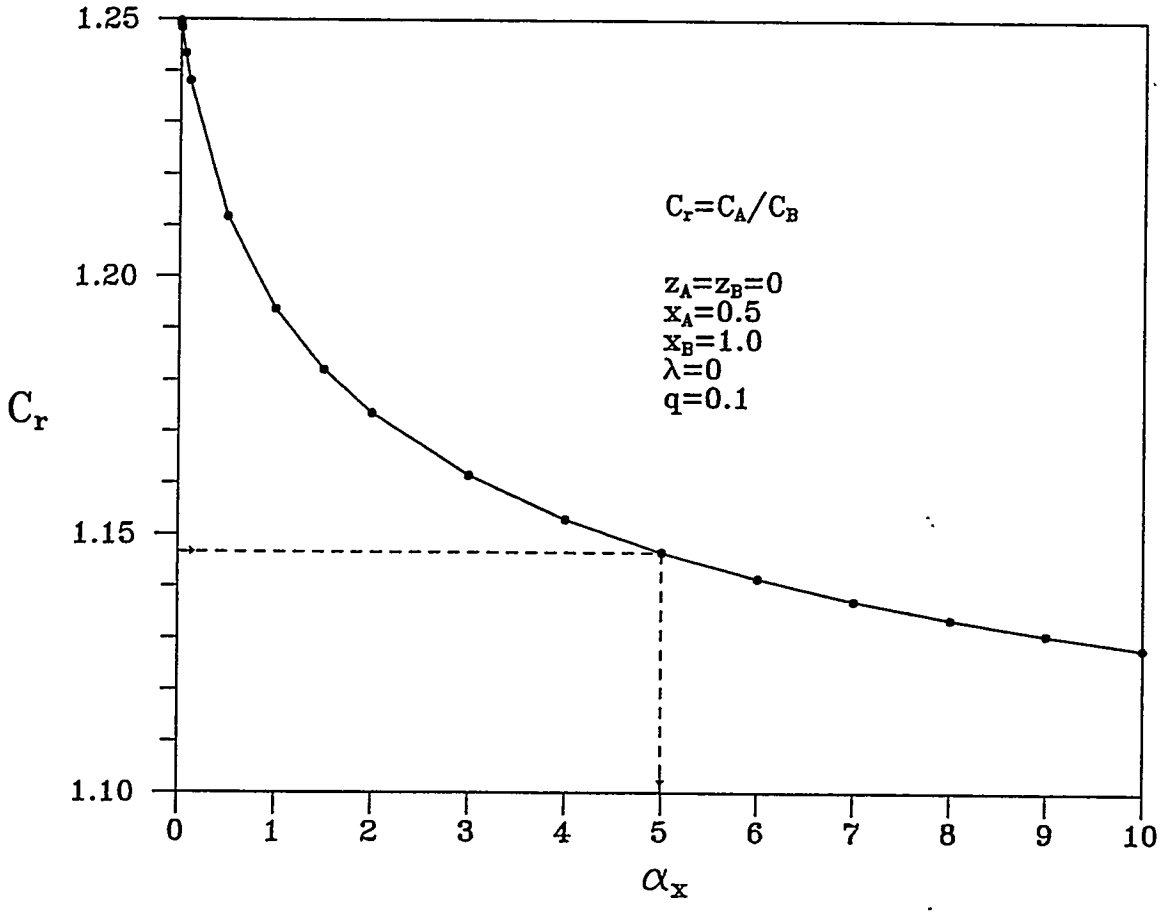

Figure 7. Steady concentration ratio between two points as a function of α_x